

CMS Paper

2010/01/13

Commissioning of the CMS Experiment and the Cosmic Run at Four Tesla

The CMS Collaboration*

Abstract

The CMS Collaboration conducted a month-long data-taking exercise known as the Cosmic Run At Four Tesla in late 2008 in order to complete the commissioning of the experiment for extended operation. The operational lessons resulting from this exercise were addressed in the subsequent shutdown to better prepare CMS for LHC beams in 2009. The cosmic data collected have been invaluable to study the performance of the detectors, to commission the alignment and calibration techniques, and to make several cosmic ray measurements. The experimental setup, conditions, and principal achievements from this data-taking exercise are described along with a review of the preceding integration activities.

arXiv:0911.4845v2 [physics.ins-det] 19 Jan 2010

*See Appendix A for the list of collaboration members

1 Introduction

The primary goal of the Compact Muon Solenoid (CMS) experiment [1] is to explore particle physics at the TeV energy scale, exploiting the proton-proton collisions delivered by the Large Hadron Collider (LHC) at CERN [2]. The complexity of CMS, like that of the other LHC experiments, is unprecedented. Therefore, a focused and comprehensive programme over several years, beginning with the commissioning of individual detector subsystems and transitioning to the commissioning of experiment-wide operations, was pursued to bring CMS into full readiness for the first LHC beams in September 2008. After the short period of beam operation the CMS Collaboration conducted a month-long data-taking exercise known as the Cosmic Run At Four Tesla (CRAFT) in late 2008. In addition to commissioning the experiment operationally for an extended period, the cosmic muon dataset collected during CRAFT has proven invaluable for understanding the performance of the CMS experiment as a whole.

The objectives of the CRAFT exercise were the following:

- Test the solenoid magnet at its operating field (3.8 T), with the CMS experiment in its final configuration underground;
- Gain experience operating CMS continuously for one month;
- Collect approximately 300 million cosmic triggers for performance studies of the CMS subdetectors.

The CRAFT exercise took place from October 13 until November 11, 2008, and these goals were successfully met.

This paper is organized as follows. Section 2 describes the detectors comprising CMS while Section 3 describes the installation and global commissioning programme prior to CRAFT. The experimental setup for CRAFT and the operations conducted are described in Sections 4 and 5, respectively, and some of the analyses made possible by the CRAFT dataset are described in Section 6.

2 Detector Description

A detailed description of the CMS experiment, illustrated in Fig. 1, can be found elsewhere [1]. The central feature of the CMS apparatus is a superconducting solenoid of 6 m internal diameter, 13 m length, and designed to operate at up to a field of 4 T. The magnetic flux generated by the solenoid is returned via the surrounding steel return yoke—approximately 1.5 m thick, 22 m long, and 14 m in diameter—arranged as a 12-sided cylinder closed at each end by endcaps. To facilitate pre-assembly of the yoke and the installation and subsequent maintenance of the detector systems, the barrel yoke is subdivided into five wheels (YB0, YB±1, and YB±2, as labeled in Fig. 1) and each endcap yoke is subdivided into three disks (YE±1, YE±2, and YE±3). Within the field volume are the silicon pixel and strip trackers, the lead tungstate crystal electromagnetic calorimeter (ECAL), and the brass-scintillator hadronic calorimeter (HCAL). Muons emerging from the calorimeter system are measured in gas-ionization detectors embedded in the return yoke.

CMS uses a right-handed coordinate system, with the origin at the nominal interaction point, the x -axis pointing to the centre of the LHC, the y -axis pointing up (perpendicular to the LHC plane), and the z -axis along the anticlockwise-beam direction. The polar angle, θ , is measured from the positive z -axis, and the pseudorapidity η is defined as $\eta = -\ln \tan(\theta/2)$. The azimuthal angle, ϕ , is measured in the x - y plane.

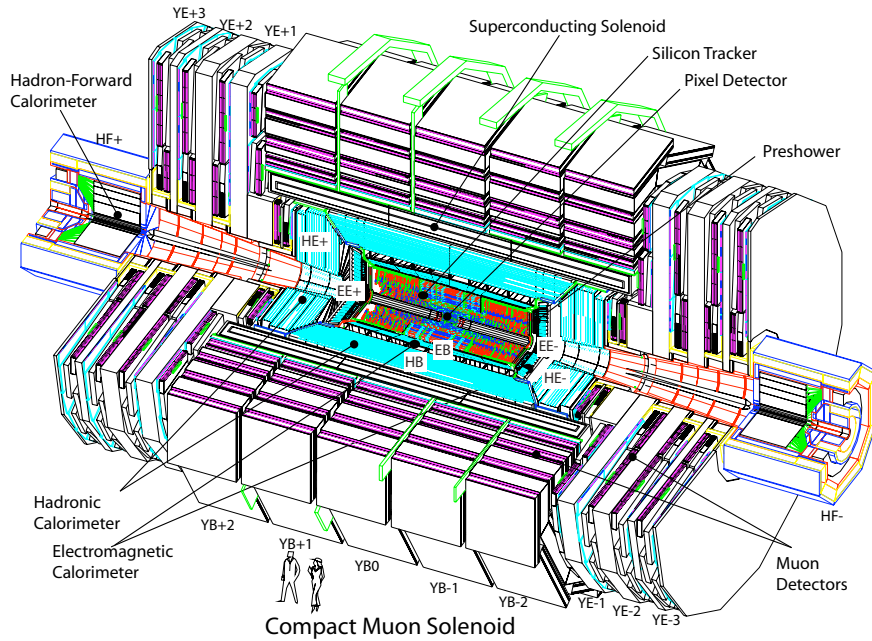


Figure 1: General view of the CMS detector. The major detector components are indicated, together with the acronyms for the various CMS construction modules.

Charged particles are tracked within the pseudorapidity range $|\eta| < 2.5$. The silicon pixel tracker consists of 1440 sensor modules containing a total of 66 million $100 \times 150 \mu\text{m}^2$ pixels. It is arranged into three 53.3 cm long barrel layers and two endcap disks at each end. The innermost barrel layer has a radius of 4.4 cm, while the other two layers are located at radii of 7.3 cm and 10.2 cm. The endcap disks extend in radius from about 6 cm to 15 cm and are located at ± 34.5 cm and ± 46.5 cm from the interaction point along the beam axis. The silicon strip tracker consists of 15 148 sensor modules containing a total of 9.3 million strips with a pitch between 80 and $180 \mu\text{m}$. It is 5.5 m long and 2.4 m in diameter, with a total silicon surface area of 198m^2 . It is constructed from six subassemblies: a four-layer inner barrel (TIB), two sets of inner disks (TID) comprising three disks each, a six-layer outer barrel (TOB), and two endcaps (TEC) of nine disks each.

The ECAL is a fine grained hermetic calorimeter consisting of 75 848 lead tungstate (PbWO_4) crystals that provide fast response, radiation tolerance, and excellent energy resolution. The detector consists of a barrel region, constructed from 36 individual supermodules (18 in azimuth per half-barrel), extending to $|\eta| = 1.48$, and two endcaps, which provide coverage up to $|\eta| = 3.0$. The crystals in the barrel have a transverse cross-sectional area at the rear of $2.6 \times 2.6 \text{cm}^2$, corresponding to $\Delta\eta \times \Delta\phi = 0.0174 \times 0.0174$, and a longitudinal length of 25.8 radiation lengths. The crystals in the endcap have a transverse area of $3 \times 3 \text{cm}^2$ at the rear and a longitudinal length of 24.7 radiation lengths. Scintillation light from the crystals is detected by avalanche photodetectors in the barrel region and by vacuum phototriodes (VPT) in the endcaps. A preshower detector comprising two consecutive sets of lead radiator followed by silicon strip sensors was mounted in front of the endcaps in 2009, after the CRAFT period, and has a thickness of three radiation lengths.

The HCAL barrel (HB) and endcaps (HE) are sampling calorimeters composed of brass and scintillator plates with coverage $|\eta| < 3.0$. Their thickness varies from 7 to 11 interaction lengths depending on η ; a scintillator “tail catcher” placed outside of the coil at the inner-

most muon detector extends the instrumented thickness to more than 10 interaction lengths everywhere. In the HB, the tower size is $\Delta\eta \times \Delta\phi = 0.087 \times 0.087$. Each HB and HE tower has 17 scintillator layers except near the interface of HB and HE. The scintillation light is converted by wavelength-shifting fibres embedded into the scintillator tiles, and is then channeled to hybrid photodiodes (HPD) via clear optical fibres. Each HPD collects signals from up to 18 different HCAL towers. The Hadron Outer (HO) calorimeter comprises layers of scintillators placed outside the solenoid cryostat to catch the energy leaking out of the HB. Its readout is identical to that of the HB and HE. Quartz fibre and iron forward calorimeters (HF), read out by photomultipliers, cover the $|\eta|$ range between 3.0 and 5.0, which corresponds to the conical central bore of each endcap yoke.

Three technologies are used for the detection of muons: drift-tubes (DT) in the central region ($|\eta| < 1.2$), cathode strip chambers (CSC) in the endcaps ($0.9 < |\eta| < 2.4$), and resistive plate chambers (RPC) throughout barrel and endcap ($|\eta| < 1.6$). The DT system comprises 250 chambers mounted onto the five wheels of the barrel yoke and arranged into four concentric “stations” interleaved with the steel yoke plates. Each chamber is built from a sandwich of 12 layers of drift tubes with 4.2 cm pitch, and is read out with multiple hit capability. Eight layers have wires along z and measure the ϕ coordinate; four layers have wires perpendicular to the z -axis and measure z (except for the outermost DT station where there are no z measuring layers). The CSC system is made of 468 chambers mounted on the faces of the endcap disks, so as to give four stations perpendicular to the beam pipe in each endcap. Each chamber has six cathode planes segmented into narrow trapezoidal strips projecting radially from the beam line, and anode wires aligned perpendicularly to the strips (wires for the highest $|\eta|$ chambers on $YE\pm 1$ are tilted by 25° to compensate for the Lorentz angle). The barrel RPC system is mounted in the same pockets in the yoke wheels as the DT system, but with six concentric layers of chambers. Each endcap RPC system consists of three layers mounted on the faces of the yoke disks. Each RPC chamber contains two gas gaps of 2 mm thickness, between which are sandwiched readout strips that measure the ϕ coordinate. The gaps work in saturated avalanche mode. The relative positions of the different elements of the muon system and their relation to reference elements mounted on the silicon strip tracker are monitored by a sophisticated alignment system.

A system of beam radiation monitors installed along the beam line gives online feedback about the beam structure and about radiation conditions within the experimental cavern [3, 4]. The main components are radio frequency (RF) pickups located ± 175 m from the interaction point, segmented scintillator rings mounted on both faces of the HF calorimeters, and diamond sensors installed very close to the beam pipe at distances of ± 1.8 m and ± 14.4 m. Signals from the diamond beam condition monitors are used to protect the tracking detectors from potentially dangerous beam backgrounds. In severe pathological conditions, they are capable of triggering an abort of the LHC beams.

Only two trigger levels are employed in CMS. The Level-1 trigger is implemented using custom hardware processors and is designed to reduce the event rate to at most 100 kHz during LHC operation using coarse information from the calorimeters, muon detectors, and beam monitoring system. It operates with negligible deadtime and synchronously with the LHC bunch crossing frequency of 40 MHz. The High Level Trigger (HLT) is implemented across a large cluster of the order of a thousand commercial computers, referred to as the event filter farm [5], and provides further rate reduction to $\mathcal{O}(100)$ Hz using filtering software applied to the full granularity data acquired from all detectors. Complete events for the HLT are assembled from the fragments sent from each detector front-end module through a complex of switched networks and “builder units” also residing in the event filter farm. The event filter farm is

configured into several “slices”, where each slice has an independent data logging element (“storage manager”) for the storage of accepted events.

3 CMS Installation and Commissioning Programme prior to CRAFT

The strategy for building the CMS detector is unique among the four major experiments for the LHC at CERN. The collaboration decided from the beginning that assembling the large units of the detector would take place in a surface hall before lowering complete sections into the underground experimental cavern. This philosophy allowed the CMS construction effort to be completed on time despite delivery of the underground cavern late in the schedule, as a result of civil-engineering works that were complicated by the geology of the terrain. Another goal was to minimize underground assembly operations which would inevitably have taken more time and would have been more complex and risky in the confined space of the cavern. Future access to the inner parts of the detector is also made easier. As construction and assembly progressed above ground, it became clear that there would be a valuable opportunity for system integration and commissioning on the surface.

3.1 The 2006 Magnet Test and Cosmic Challenge

The large solenoid of CMS was first fully tested while it was in the surface assembly hall during August–November 2006. This provided the opportunity to test the integration of major components of the experiment before lowering them into the underground experimental cavern, and slices of the major detector subsystems were prepared to record data concurrently with this test. The exercise, called the Magnet Test and Cosmic Challenge (MTCC), provided important commissioning and operational experience, and was the precursor of the CRAFT exercise described in this paper. The magnetic field was increased progressively up to its maximum operating value of 4.0 T, and fast discharges were commissioned such that 95% of the operating current of 19 140 A (corresponding to 2.6 GJ of stored energy) could be dumped in a time span of about 10 minutes. Distortions of the yoke during the testing were monitored by the muon alignment system [6], which was installed in one endcap and in an azimuthal slice of the barrel across all wheels. After the successful completion of testing in the surface hall in 2006, the magnet and its main ancillary systems were moved to their final positions in the service and experimental caverns and nearby surface installations.

Concurrently with the first phase of the 2006 magnet test, about 7% of the muon detection systems, 22% of HCAL, 5% of ECAL, a pilot silicon strip tracker (about 1% of the scale of the complete tracker), and the global trigger and data acquisition were successfully operated together for purposes of globally commissioning the experiment and for collecting data to ascertain the detector performance. For the second phase of the exercise, the ECAL and pilot tracker were removed and the central magnetic field was mapped with a precision of better than 0.1%, using a specially designed mapping carriage employing Hall probes mounted on a rotating arm [7], for several operating fields of the magnet. These maps are now used in the offline simulation and reconstruction software. In total, approximately 200 million cosmic muon events were recorded for purposes of calibration, alignment, and detector performance studies using this slice of the experiment while on the surface. The conclusion of MTCC coincided with the start of the installation into the underground cavern.

The MTCC was an opportunity to uncover issues associated with operating the experiment with the magnetic field at its design value. One effect seen was the susceptibility of the hybrid photodetectors (HPD) used to read out the scintillation light from the HCAL: the noise rate from these devices depends on the magnetic field, and is maximal in the range 1–2 T. At the

design value of 4 T the noise rate was found to be acceptable for the barrel and endcap compartments of HCAL; but for the Hadron Outer “tail catcher” in the barrel, whose HPDs are mounted in pockets in the return yoke where the magnitude of the field is lower, the noise rate was unacceptably high and the tubes had to be repositioned.

3.2 Installation of CMS Components Underground

The heavy elements of CMS began to be lowered into the experimental cavern in November 2006, starting with the forward calorimeters and continuing shortly thereafter with the $+z$ endcap disks and barrel wheels, complete with muon detectors and services. The central yoke wheel (YB0), which houses the cryostat, was lowered in February 2007, and by January 2008 the last heavy elements of the $-z$ endcap were successfully lowered into the cavern.

The campaign to connect services for the detectors within the central portion of CMS included the installation of more than 200 km of cables and optical fibres (about 6000 cables). Additionally, more than 20 km of cooling pipes (about 1000 pipes) were installed. The whole enterprise took place over a 5 month period and required more than 50 000 man-hours of effort. The cabling of the silicon strip tracker was completed in March 2008, and its cooling was operational by June 2008. In the same month, the central beam pipe, which is made of beryllium, was installed and baked out (heated to above 200 °C while under vacuum for approximately a week).

The silicon pixel tracking system and the endcaps of the ECAL were the last components to be installed, in August 2008. The mechanics and the cabling of the pixel system have been designed to allow relatively easy access or replacement if needed. The preshower detector for the endcap electromagnetic calorimeter was the only major subsystem not installed prior to the 2008 LHC run and the CRAFT exercise. It was installed in March 2009.

3.3 Global Run Commissioning Programme

A series of global commissioning exercises using the final detectors and electronics installed in the underground caverns, each lasting 3–10 days and occurring monthly or bimonthly, commenced in May 2007 and lasted until the experiment was prepared for LHC beams, by the end of August 2008. These “global runs” balanced the need to continue installation and extensive detector subsystem commissioning with the need for global system tests. The scale of the global runs is illustrated in Fig. 2, which shows, as a function of time, the effective fraction of each of the seven major detector systems participating in the run (excluding the ECAL preshower system). Generally, the availability of power, cooling, and gas limited the initial scope of the commissioning exercises; by the time of the November 2007 global run, however, these services were widely available.

Many detector subsystems were available in their entirety for global commissioning by May 2008, and thus a series of four week-long exercises, each known as a Cosmic RUn at ZERo Tesla (CRUZET), were conducted to accumulate sizable samples of cosmic muon events from which to study the overall detector performance. Notable for the third CRUZET exercise, in July 2008, was the introduction of the silicon strip tracker into the data-taking (with about 75% of the front-end modules). In the fourth CRUZET exercise, in August 2008, the complete silicon pixel tracker was introduced, along with the endcaps of the ECAL. In addition to the operational experience of the exercises and the ability to address more subtle detector performance issues with larger event samples, the data were critical for deriving zero-field alignment constants for the inner tracking systems. Several detector studies using CRAFT data also made use of these CRUZET data samples. The total accumulated cosmic triggers at zero field exceeded 300

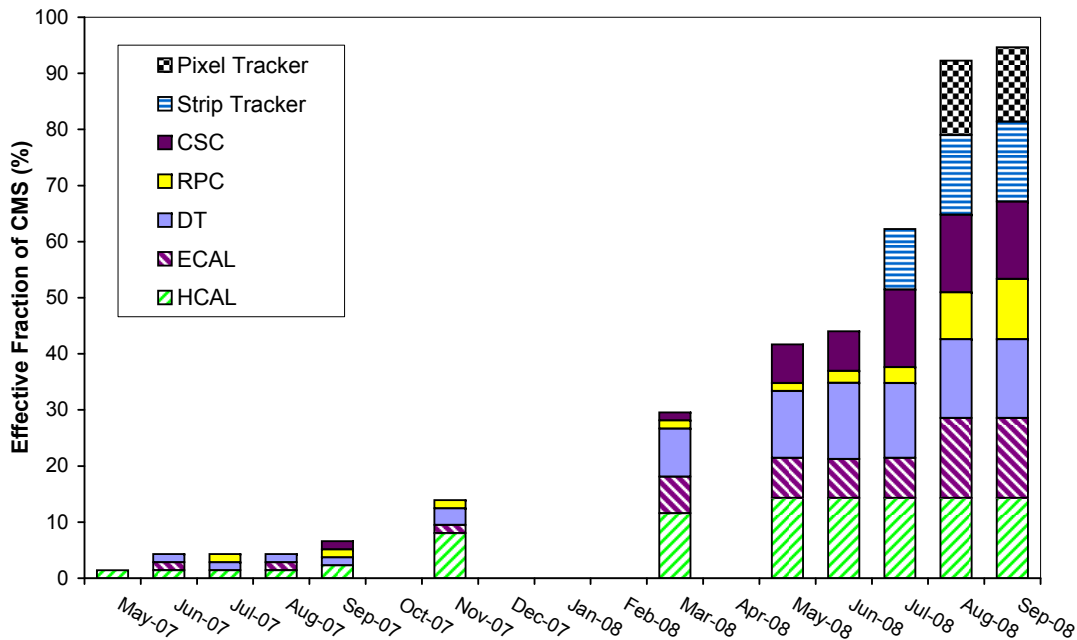


Figure 2: Effective fraction of the CMS experiment participating in the 2007 and 2008 global run campaigns as a function of time. The fraction of each of the seven major detector systems is represented by a bar with a length of up to $\frac{1}{7} \cdot 100\%$. Only one RPC endcap was missing by September 2008.

million, including the triggers recorded in September 2008 when the experiment was live for the first LHC beams.

These global runs regularly exercised the full data flow from the data acquisition system at the experimental site to the reconstruction facility at the CERN IT centre (called the Tier-0 centre), followed by the subsequent transfer of the reconstructed data to all seven of the CMS Tier-1 centres and to some selected Tier-2 centres [8].

3.4 Final Closing of CMS

The final sequence of closing the steel yoke and preparing CMS for collisions was completed on August 25, 2008 (see Fig. 3). This was followed by several tests of the solenoid in the underground cavern for the first time, up to a field of 3 T, as described further in Section 5.2. The final test at the operating field was postponed until CRAFT due to the imminent arrival of beam at the beginning of September and the necessity of keeping the solenoid off for the initial commissioning phase of the LHC.

3.5 LHC Beam Operations in 2008

The CMS experiment was operational and recorded triggers associated with activity from the first LHC beams in September 2008. This activity included single shots of the beam onto a collimator 150 m upstream of CMS, which yielded sprays (so-called “beam splashes”) containing $\mathcal{O}(10^5)$ muons crossing the cavern synchronously, and beam-halo particles associated with the first captured orbits of the beam on September 10 and 11.

The configuration of the experiment for LHC beam operations was nearly the same as that for

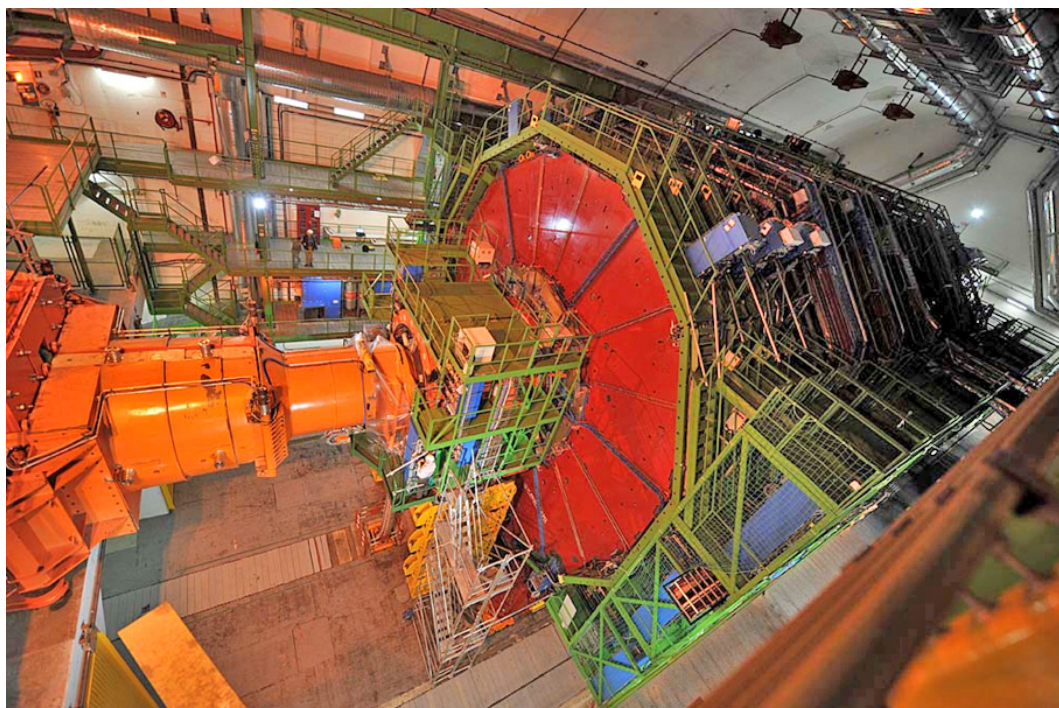


Figure 3: The CMS experiment in its final, closed configuration in the underground experimental cavern.

CRAFT. The exceptions were that the silicon pixel and strip tracking systems were powered off for safety reasons, time delays in the readout electronics between the top and bottom halves of the experiment were removed, and the Level-1 trigger menu was set for synchronous beam triggers.

The first “beam splash” events were used to synchronize the beam triggers, including those from the RF beam pick-ups, the beam scintillation counters surrounding the beam pipe, the forward hadron calorimeters, and the CSC muon system. The diamond beam condition monitors were also commissioned with beam, providing online diagnostics of the beam timing, bunch structure, and beam-halo. The data collected from the “beam splash” events also proved useful for adjusting the inter-channel timing of the ECAL [9] and HCAL [10] readout channels, as the synchronous wave of crossing muons has a characteristic time-of-flight signature.

In total, CMS recorded nearly 1 million beam-halo triggered events during the 2008 beam operations.

4 Experiment Setup for CRAFT

4.1 Detector Components

All installed detector systems were available for testing during CRAFT. The silicon pixel tracker and the ECAL endcaps were the last major systems to be installed and thus were still being commissioned and tuned even after the start of CRAFT. Furthermore, the commissioning of the RPC system had been delayed by the late delivery of power supplies; and by the time of CRAFT the RPC endcap disks were not yet commissioned for operation.

4.2 Trigger and Data Acquisition

The typical Level-1 trigger rate during CRAFT was 600 Hz. This rate is well below the 100 kHz design limit for the central data acquisition (DAQ) system and is composed of about 300 Hz of cosmic triggers using all three muon systems, 200 Hz of low threshold triggers from the calorimeters, and 100 Hz of calibration triggers used to pulse the front-end electronics or to illuminate the optical readout paths of the calorimeters. The cosmic muon triggers were more permissive than what would be used during collisions, with only loose requirements for the muon to point to the interaction region of the experiment. The rate of triggered cosmic muons crossing the silicon strip tracker region was $\mathcal{O}(10)$ Hz. As CMS is located 100 m below the surface of the Earth, the cosmic muon rate relative to that at the surface is suppressed by approximately two orders of magnitude. The time-of-flight of cosmic muons to cross from the top to the bottom of the experiment was accounted for by introducing coarse delays of the muon trigger signals in the top half such that they are in rough coincidence with the bottom half (a two bunch crossing difference for the barrel, and one for the endcaps, where one bunch crossing corresponds to 25 ns). The calorimeter triggers were configured with low thresholds selecting mostly detector noise. Further details on the configuration and performance of the Level-1 trigger during CRAFT can be found in Ref. [11].

The event filter farm was configured into four “slices”. There were 275 builder units that assembled the data fragments into complete events, and 825 filter units for HLT processing. The average size of an event built by the DAQ during CRAFT is about 700 kB. The HLT primarily applied only pass-through triggers with no filtering, in order to efficiently record cosmic ray events selected by the Level-1 trigger, although additional complex filters were phased in for physics selection, alignment and calibration of the detector, and diagnostics [12]. At the end of CRAFT, a DAQ configuration with eight slices and nearly 4500 filter units was successfully tested.

5 Operations

5.1 Control Room Operations and Tools

Control room operations for CMS, as executed during CRAFT, are carried out by a five-person central shift crew responsible for the global data-taking of the experiment, and 10–14 subsystem shifters responsible for the detailed monitoring and control of specific detector systems during this commissioning period. These operations are in general conducted continuously, necessitating three shift crews daily.

The central shift crew is composed of a shift leader, a detector safety and operation shifter, a DAQ operator, a trigger control operator, and a data quality monitoring (DQM) shifter. The shift leader is responsible for the overall safety of the experiment and personnel, and for the implementation of the run plan as set by the run coordinators.

The DAQ operator issues the sequence of commands for initializing the detector readout electronics and controls the data-taking state via the run control system. Several displays are devoted to monitoring the state of the DAQ system and for detailed diagnostics. The trigger operator is responsible for the monitoring of the Level-1 trigger system and for configuring the system with the desired settings (the participating trigger components, delays, etc.).

The central DQM shifter in the control room uses the CMS-wide DQM services [8], monitoring event data to assess the quality of the data collected during a run. The DQM shifter is responsible for certifying runs for data analysis purposes. This information is entered into a

“run registry” database (which also contains configuration information about the run), and forms the first step in a chain that assigns quality flags on a subsystem-by-subsystem basis. The information was used to select event samples, such as those used in the studies of the detector performance during CRAFT. The control room DQM shifter is assisted by another shifter located at one of the remote operations centres (Fermilab and DESY).

Additional information available to the central and detector shifters to assess the detector status includes the notification of any alarm triggered by the detector safety system, such as cooling or power failures, and monitoring data from the Detector Control System (DCS) such as temperature readings from the detector and electronic components, the status of the cooling plants, the status of the high and low voltage power, etc. The DCS system is accessible from within the online network, and graphical interfaces have been developed for use in the control room. As the detector status data are stored in a database, a set of software tools, known as Web-Based Monitoring (WBM), was also designed to extract and display the information inside and outside the control room network. Both real-time status data and historical displays are provided. Example WBM applications are: Run Summary (detailed information about the runs taken), DCS information (current condition and past history of each subdetector component), magnet variables, and trigger rates. These WBM applications were used extensively during the CRAFT data-taking operation as well as during the subsequent analysis stage to understand the data-taking configurations and conditions.

5.2 Magnet Operations

The operating current for the solenoid was set to 18 160 A ($B = 3.8$ T), although the magnet has been successfully tested to its design current of 19 140 A ($B = 4.0$ T) as noted in Section 3.1. This choice for the initial operating phase of the experiment was made to have an additional safety margin, with little impact on physics measurements, in view of the long period of operation that is expected to exceed 10 years.

The magnet operated successfully for the duration of CRAFT. Nominal performance was achieved in the control racks, safety system, cryogenic system, and passive protection system. Apart from a ramp-down to allow access to the experimental cavern during the LHC inauguration, the only interruptions of the magnet were due to water cooling interlocks caused by an incorrectly adjusted leak-detection threshold.

The magnet was at its operating current for the CRAFT exercise for a total of 19 days, between October 16 and November 8, 2008, as illustrated in Fig. 4. Ramping tests indicate a nominal time of 220 minutes for magnet rampings (up or down), keeping the magnet at a temperature of 4.5 K. Distortions of the yoke during ramps were measured by the muon alignment systems (Section 5.4.5).

Shortly after the CRAFT data-taking exercise at 3.8 T ended, a final ramp was made to 4.0 T on November 14 to ensure the magnet stability margin. After bringing the field back to 3.8 T, a fast discharge was triggered, which took only 10 minutes. The final average temperature of the magnet after a fast discharge is 66 K, requiring at least three days to reestablish the operating temperature.

5.3 Infrastructure

The infrastructure and services met the demands of running the experiment continuously for one month, although the exercise indicated areas needing further improvement. No particular problem or malfunction of the electrical and gas distribution systems for the experiment occurred during CRAFT. Likewise, the nitrogen inerting and dry air systems, intended to pre-

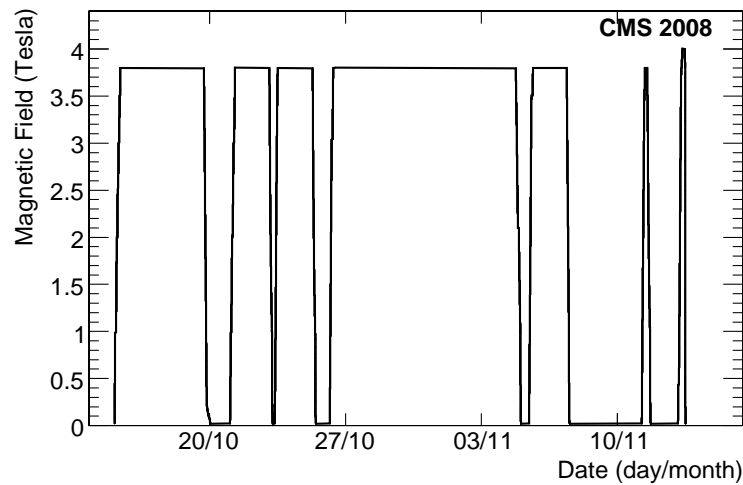


Figure 4: History of the magnitude of the central magnetic field during CRAFT. The ramp-down on October 20 was needed to allow open access to the experimental cavern. The last two ramp-ups in November were further tests of the magnet after CRAFT data-taking.

vent fire and guarantee a dry atmosphere in humidity sensitive detectors, operated stably. The detector safety and control systems performed as expected, but further functionality and testing took place after CRAFT.

Several cooling failures did occur, and this resulted in the shutdown of some equipment during CRAFT. One circulating pump failed due to a faulty installation. Leaks were detected on the barrel yoke circuit for wheels YB-2 and YB-1. As noted earlier, the leak detection system on one of the cooling circuits fired a few times resulting in three separate automatic slow dumps of the magnet (leading to at least 8 hours loss at 3.8 T). The threshold has been subsequently raised to make the system more robust.

The cooling plants for the silicon strip tracker suffered a few trips, leading to about 6 hours down-time during CRAFT. The leak rate of the system was also higher than expected. In the shutdown after CRAFT, the cooling plants and piping were significantly refurbished to eliminate these leaks.

In total, about 70 hours of downtime were caused by general infrastructure related incidents, about 10% of the duration of CRAFT. This time was dominated by the downtime of the magnet.

5.4 Detector Operations

The operational performance of the detector subsystems during CRAFT is reported in detail in Refs. [13]–[19]. All detector systems functioned as intended in the 3.8 T magnetic field. Here we summarize the principal operations conducted during CRAFT and the main observations.

5.4.1 Tracker

The silicon strip tracker [13] was live 95% of the running time during CRAFT, with 98% of the channels active. Signals were collected via a 50 ns CR-RC shaper, sampled and stored in an analog pipeline by the APV25 front-end chip [20]. The APV25 chip also contains a deconvolution circuit, not used during CRAFT, to reduce the signal width (but increasing the noise) that can be switched on at high LHC luminosity, when pile-up becomes an issue. The tracker readout was synchronized to triggers delivered by the muon detectors. A few issues not identified

during the previous commissioning of the detector, such as some swapped cables and incorrect fibre length assumptions used in the latency calculations, were quickly identified by offline analysis of the cosmic data and corrected either during operation or the subsequent shutdown. Data were zero suppressed during the entire exercise. The signal-to-noise ratio was excellent, ranging from 25 to more than 30 depending on the partition, after final synchronization adjustments.

The silicon pixel tracker [14] was live 97% of the running time. In the barrel pixel system, 99% of the channels were active, whereas in the forward pixel system 94% were active. The 6% inactive channels in the latter were mostly due to identified shorts in the power supply cables, which were repaired during the subsequent shutdown. Zero suppression was performed on the detector, with conservative thresholds of about 3700 electrons chosen to ensure stable and efficient operations during CRAFT. The pixels were mostly immune to noise, with a noisy channel fraction of less than 0.5×10^{-5} . The mean noise from the front-end readout chips in the barrel and forward detectors is 141 and 85 electrons, respectively, well below the operating thresholds.

5.4.2 ECAL

For the ECAL [15], the fraction of channels that were operational during CRAFT was 98.5% in the barrel and 99.5% in the endcaps. A large part of the barrel inefficiency was due to a cut power cable that has since been repaired. In the barrel, approximately 60% of the dataset was recorded with nominal front-end electronics gain while the other 40% was recorded with the gain increased by a factor of 4, to enhance the muon signal.

The response of the ECAL electronics, both in the barrel and in the endcap, was monitored using pulse injections at the preamplifier, showing no significant changes due to the magnetic field. Noise levels were generally consistent with the values measured during construction, aside from a small increase for 1/4 of the barrel that is believed to be low frequency pickup noise associated with the operation of other CMS subdetectors and that is mostly filtered by the amplitude reconstruction algorithm.

The temperature of the ECAL is required to be stable at the level of 0.05°C in the barrel and 0.1°C in the endcaps in order to ensure that temperature fluctuations remain a negligible contribution to the energy resolution (both crystal light yield and barrel front-end gain are temperature dependent). The stability provided by the temperature control system during CRAFT was measured to be about 0.01°C for the barrel and 0.05°C in the endcaps, with almost all measurements better than the required specifications.

The ECAL barrel high voltage should also be kept stable at the level of a few tens of mV due to the strong gain dependence of the photodetector on the absolute voltage value (3% per volt). The average fluctuation of the high voltage is measured to be 2.1 mV (RMS), with all channels within 10 mV.

A laser monitoring system is critical for maintaining the stability of the constant term of the energy resolution at high luminosities. Its main purpose is to measure transparency changes for each crystal at the 0.2% level, with one measurement every 20–30 minutes. During CRAFT, a total of approximately 500 sequences of laser monitoring data were taken, with each sequence injecting 600 laser pulses per crystal. These data were collected using a calibration trigger issued in the LHC abort gap at a rate of typically 100 Hz. The measured stability was better than the 0.2% requirement for 99.9% of the barrel and 99% of the endcap crystals.

To stabilise the response of the endcap VPTs, which have a rate-dependent gain (5–20% vari-

ation in the absence of magnetic field, and significantly reduced at 3.8 T [15]), an LED pulsing system was designed to continuously pulse the VPTs with a rate of at least 100 Hz. This system was successfully tested during CRAFT on a small subset of channels, and LED data were acquired in different configurations.

5.4.3 HCAL

HCAL participated in the CRAFT data-taking with all components: barrel (HB), endcap (HE), forward (HF) and outer (HO) calorimeters [16]. The fraction of non-operational channels overall for HB, HE and HF was 0.7% (0.5% due to noisy HPDs in HB and HE, and 0.2% to electronics failures), while for HO it was about 4.5% (3.3% due to noisy HPDs and 1.2% to electronics) at the start of CRAFT and increased to 13% due to HPD failures as noted below.

As found during the MTCC exercise, the HPD noise rate depends on the magnetic field. Therefore, the behaviour of all HPDs was carefully monitored during CRAFT to identify those HPDs that failed, or were likely to fail, at 3.8 T in order to target them for replacement. Noise data from HB and HE were collected using a trigger with a threshold of 50 fC that is approximately equivalent to 10 GeV of energy. Based on individual HPD discharge rates, the high voltage to four HPDs on HB and HE (out of 288 total) was reduced during CRAFT from 7.5 to 6.0 kV (which lowers the gain by approximately 30%), in addition to two HPDs that were completely turned off. At 3.8 T the resulting measured trigger rate from 286 HPDs in HB and HE was approximately 170 Hz, which can be compared to the rate at zero field of about 130 Hz. The HPDs of HB and HE showed no signs of increased noise rates during CRAFT.

The HO HPDs servicing the central wheel (YB0) operate in a fringe field of 0.02 T (when the central field of the magnet is 3.8 T) while those on the outer wheels (YB \pm 1, YB \pm 2) experience a magnetic field above 0.2 T. While no HPDs on YB0 showed any significant discharge rate, it was expected from the MTCC experience that several HPDs on the outer wheels would, and this was observed. Twenty HPDs installed on the outer wheels at the start of CRAFT showed significant increase in the noise rates at 3.8 T with respect to the noise rates at 0 T. The high voltage was turned off for the four HPDs with the highest noise rate increases, and was lowered to 7 kV for the others. The HO HPDs located on the outer wheels showed clear signs of increased discharge rates during CRAFT. As the number of discharging HPDs continued to increase, the high voltage on all HPDs servicing the outer wheels was further lowered to 6.5 kV midway into CRAFT. By the end of the run, a total of 14 HPDs were turned off out of 132 for all of HO.

During the winter 2008/09 shutdown, after CRAFT, the problematic channels were fixed, including replacing HPDs with anomalously high noise rates or low gains. A total of 19 HPDs were replaced in HB and HE, and another 19 in the HO outer wheels. As of November 2009, after additional tests with the magnetic field, all of the HB, HE, and HF channels were operational while the number of non-operational channels in HO was at the level of 4%.

5.4.4 Muon Detectors

The DT system had all 250 chambers installed, commissioned and equipped with readout and trigger electronics for CRAFT, and 98.8% of the channels were active. The DT trigger was operated in a configuration requiring the coincidence of at least two nearby chambers without requiring that the muon trajectory points to the nominal interaction point. The cosmic trigger rate for this configuration was stable at about 240 Hz. The performance of the DT trigger is described in more detail in Ref. [17].

The DT system demonstrated high reliability and stability. Some noise was observed sporad-

ically during the period when the field was on. In particular, synchronous noise produced huge events, with high occupancy in the detectors comprising the wheels on one side of the experiment, at the level of 0.1–1 Hz. Noise sources are under investigation.

The RPC system participated in CRAFT with the entire barrel and a small fraction of the endcaps [18], which at the time were at an early stage of commissioning. For the barrel part, the CRAFT operation was important to ascertain the system stability, debug the hardware, synchronize the electronics, and ultimately obtain a preliminary measurement of the detector performance. About 99% of the barrel electronic channels were active during the data taking, while the remaining 1% were masked due to a high counting rate. The average cosmic muon RPC trigger rate was about 140 Hz for the barrel, largely coincident with the DT triggers, with some spikes in rate as noted below.

The main RPC monitoring tasks ran smoothly during the entire period, which allowed a careful analysis of system stability. The average current drawn by the barrel chambers (each having a 12 m² single gap surface) was stable below 1.5 μ A, with very few cases above 3 μ A. A study of the chamber efficiency as a function of the operating voltage was possible for about 70% of the barrel chambers, giving a preliminary estimate of the average intrinsic detector efficiency of about 90%. This study also indicated a few hardware failures and cable map errors that were later fixed.

Sporadic RPC trigger spikes related to noise pick-up from external sources were also detected. The sensitivity of the system to these sources is under investigation. However, preliminary studies have demonstrated that the trigger rate is almost unaffected when the standard trigger algorithm for LHC collisions is applied.

The CSC system operated with more than 96% of the readout channels active and for about 80% of the CRAFT running period [19]. The rate of trigger primitive segments in the CSCs from cosmic-ray muons underground was about 60 Hz, distributed over the two endcaps. The CSC trigger was configured to pass each of these trigger segments, without a coincidence requirement, as muon candidates to the Level-1 Global Trigger.

The long running period under stable conditions provided by CRAFT exposed a few issues that had not yet been encountered during the commissioning of the CSCs. These effects include a very low corruption rate of the non-volatile memories used to program some FPGAs distributed in the system, and unstable communication with the low voltage power supplies. Actions taken after CRAFT to address these issues included periodic refreshing of the memories and a replacement of the control signal cables to the power supplies, respectively.

5.4.5 Muon Alignment System

The complete muon alignment system was tested during CRAFT [21]. It is organized into three main components: two local systems to monitor the relative positions of the DT and CSC muon detectors separately, and a “link system” that relates the muon chambers and central tracker and allows simultaneous monitoring of the barrel and endcap. All components are designed to provide continuous monitoring of the muon chambers in the entire magnetic field range between 0 T and 4 T. The acquisition of data from these systems is separate from the central DAQ used to collect normal event data.

Each DT chamber is equipped with LEDs as light sources, and about 600 video cameras mounted on rigid carbon-fibre structures observe the motions of the chambers. During the CRAFT data taking period, as well as the periods just before and after, over 100 measurement cycles were recorded. Compression of the barrel wheels in z with the magnet at 3.8 T was observed at

the level of 1–2 mm depending on azimuth, and with an uncertainty of 0.3 mm, in agreement with previous measurements made during MTCC.

The acquisition of endcap alignment data was robust, and 99.4% of the sensors were operational. The sensors monitor displacements from reference laser beams across each endcap disk, and provide positioning information on 1/6 of the endcap chambers. This allows adequate monitoring of the yoke disk deformations due to strong magnetic forces. The measurements with the magnet at 3.8 T indicate deformations of all disks towards the interaction point by about 10–12 mm for chambers close to the beam line and by about 5 mm for chambers further away. These results are consistent with earlier MTCC measurements.

The link system comprises amorphous silicon position detectors placed around the muon spectrometer and connected by laser lines. The complete system was implemented for CRAFT, and 98% operational efficiency was obtained. Unfortunately, the closing of the YE–1 disk outside of its tolerance created a conflict with some of the alignment components, making the laser system for this part of the detector effectively unusable during CRAFT. The disk could not be repositioned given the limited remaining time to prepare CMS for LHC beams in 2008. Consequently, full reconstruction of the link system data was possible only for the +z side of the detector. During CRAFT, data were recorded at stable 0 T and 3.8 T field values, as well as during magnet ramps. Information from the link system was used to align CSCs on $YE\pm 1$. Both the endcap alignment and the link system detected disk bending, and CSC tilts were measured at full field.

5.5 Data Operations

The average data-taking run length during CRAFT was slightly more than 3 hours, and four runs exceeded 15 hours without interruption (one run exceeded 24 hours). Reasons for stopping a run included the desire to change the detector configuration, a hardware-related issue with a detector subsystem (e.g. loss of power), some part of the readout electronics entering an irrecoverable busy state, or other irrecoverable DAQ system errors. Aside from the 10% downtime due to infrastructure related problems, the typical data collection efficiency of CMS was about 70% during CRAFT, including periods used to conduct detector calibrations, pedestal runs, and diagnostics to further advance the commissioning of the experiment. The breakdown of the total number of collected events passing quality criteria for the detector systems or combination of systems, but not necessarily with a cosmic muon within its fiducial volume, is listed in Table 1. Figure 5 shows the accumulated number of cosmic ray triggered events as a function of time with the magnet at its operating central field of 3.8 T, where the minimal configuration of the silicon strip tracker and the DT muon system delivering data certified for further offline analysis was required. It was not required to keep the other systems in the configuration. A total of 270 million such events were collected. The effective change in slope after day 18 is principally due to downtime to further improve the synchronization of the silicon strip tracker and an unplanned ramp-down of the magnet.

Data were promptly reconstructed at the Tier-0 computing centre at CERN to create high-level physics objects with a job latency of about 8 hours, but with a broad distribution. These data were transferred to the CMS Analysis Facility (CAF) at the CERN Meyrin site and to several Tier-1 and Tier-2 centres worldwide for prompt analysis by teams of physicists. The average export rate from the Tier-0 centre to the Tier-1 centres during CRAFT was 240 MB/s, and the total volume transferred was about 600 TB. Data quality monitoring of the Tier-0 reconstruction output in addition to the standard online monitoring at the control room was provided. Specialized data selections for detector calibration and alignment purposes also were created

Table 1: The number of cosmic ray triggered events collected during CRAFT with the magnetic field at its operating axial value of 3.8 T and with the listed detector system (or combination of systems) operating nominally and passing offline quality criteria. The minimum configuration required for data-taking was at least one muon system and the strip tracker. The other subdetectors were allowed to go out of data-taking for tests.

Detector	Events (millions)
Pixel Tracker	290
Strip Tracker	270
ECAL	230
HCAL	290
RPC	270
CSC	275
DT	310
DT+Strip	270
All	130

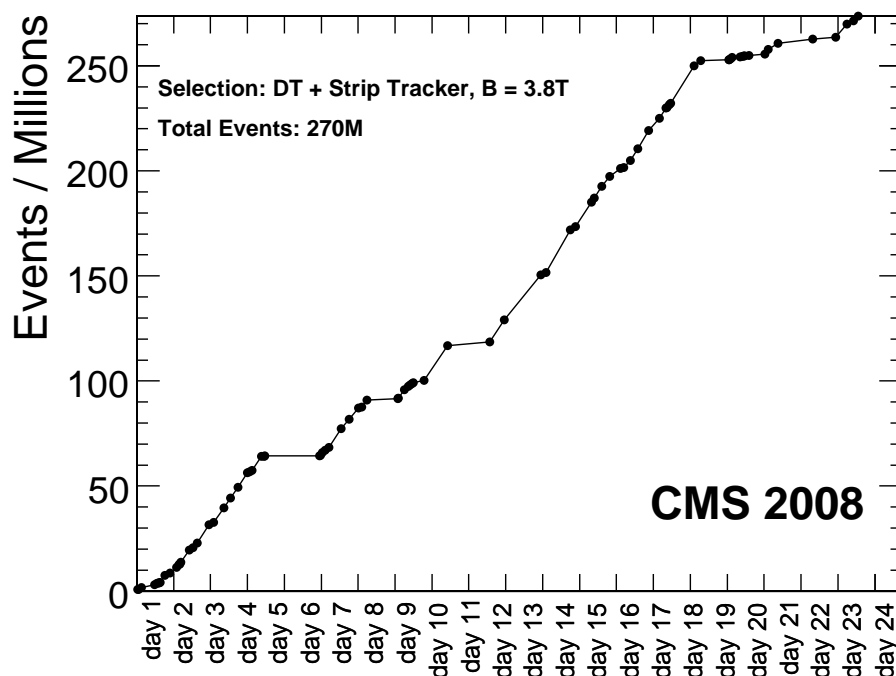


Figure 5: The accumulated number of good (see text) cosmic ray triggered events with the magnet at 3.8 T as a function of days into CRAFT, beginning October 16, 2008.

from the Tier-0 processing, and they were processed on the CAF to update the alignment and calibration constants. Several reprocessings of the CRAFT datasets took place at the Tier-1 centres using the refined calibration and alignment constants after the CRAFT data taking period. For ease of offline analyses, several primary datasets were produced that were derived from dedicated HLT filters. Some datasets were further reduced, selecting for example events enriched in the fraction of cosmic muons pointing to the inner tracking region of the experiment. Further details on the offline processing workflows applied to the CRAFT data are described in Ref. [8].

5.6 Lessons

The extended running period of CRAFT led to the identification of some areas needing attention for future operations. As noted in a few instances already, some repairs or replacements of detector subsystem components were required, such as the repair of several power cables to the pixel tracker, the replacement of some HPDs for the HCAL, and the replacement of some muon electronics on the detector. The cooling plants for the silicon tracking systems were refurbished to eliminate leaks in the piping, and improved water leak detection was added to the barrel yoke. Based partly on the experience of CRAFT, the complexity of the HLT menu to be used for initial LHC operations was reduced and some algorithms were improved for better CPU and memory usage performance.

In order to measure the efficiency of data-taking automatically and to systematically track the most significant problems, a tool was developed after CRAFT to monitor the down-times during data-taking and the general reasons for each instance (as selected by the shift leader). In an effort to improve the efficiency, further centralization of operations and additional alarm capability were added to the detector control and safety systems. More stringent change-control policies on hardware interventions, firmware revisions, and software updates were also enacted during subsequent global-taking periods in order to further limit any unannounced changes.

Many CRAFT detector analyses successfully used the computing facilities of the CAF, but to the extent that it became clear afterward that the disk and CPU usage policies needed refinement. One unexpected outcome from the CRAFT analyses was the identification of a problem in the initial calculation of the magnetic field in the steel yoke for the barrel that became evident when studying cosmic muons recorded during CRAFT (see Section 6).

6 Detector Performance Studies

The data collected during CRAFT, with CMS in its final configuration and the magnet energized, facilitated a wide range of analyses on the performance of the CMS subdetectors, the magnitude of the magnetic field in the return yoke, as well as the calibration and alignment of sensors in preparation for physics measurements. Figure 6 shows a transverse view of the CMS experiment with the calorimeter energy deposits and tracking hits indicated from one cosmic muon traversing the central region during CRAFT. It also shows the results of the muon trajectory reconstruction.

Alignment of the silicon strip and pixel sensor modules was improved significantly from initial survey measurements by applying sophisticated track-based alignment techniques to the data recorded from approximately 3.2 million tracks selected to cross the sensitive tracking region (with 110 000 tracks having at least one pixel hit). The precision achieved for the positions of the detector modules with respect to particle trajectories, derived from the distribution of the me-

2008-Oct-20 04:52:41.749892 GMT: Run 66748, Event 8868341, LS 160, Orbit 166856666, BX 2633

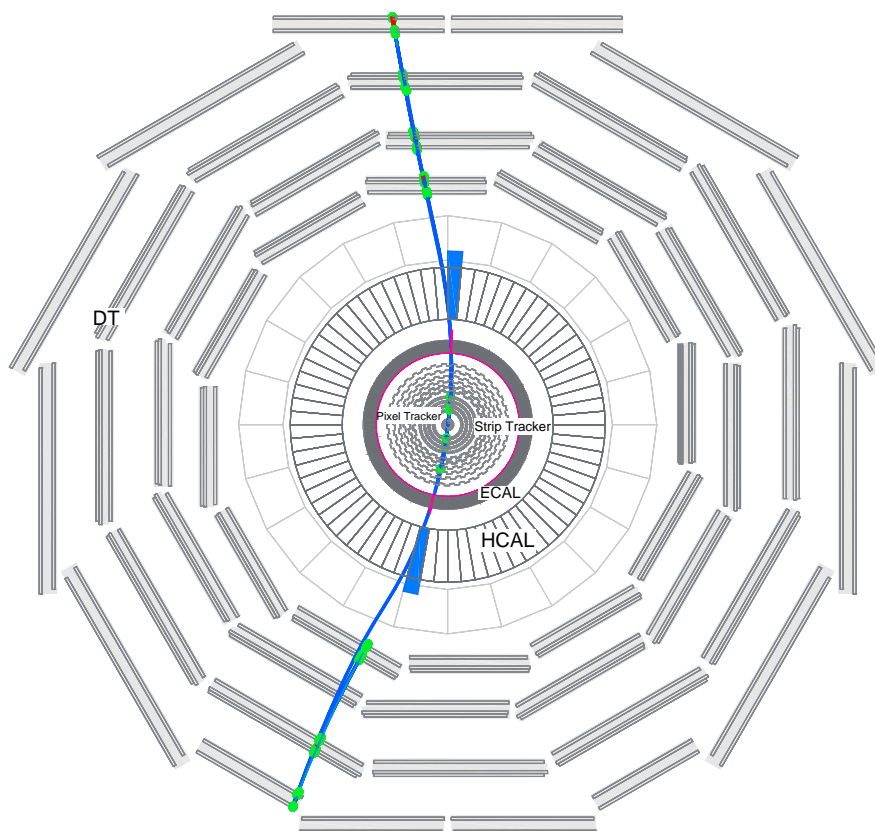


Figure 6: Display of a cosmic muon recorded during CRAFT which enters and exits through the DT muon system, leaves measurable minimum ionizing deposits in the HCAL and ECAL, and crosses the silicon strip and pixel tracking systems. Reconstruction of the trajectory is also indicated.

dian of the cosmic muon track residuals, is 3–4 μm in the barrel and 3–14 μm in the endcaps for the coordinate in the bending plane [22]. Other silicon tracking measurements [13] performed with the CRAFT data include calibration of the absolute energy loss in silicon strip sensors, Lorentz angle measurements, hit efficiencies and position resolutions, track reconstruction efficiencies, and track parameter resolutions. The efficiency of reconstructing cosmic ray tracks, for example, is greater than 99% for muons passing completely through the detector and close to the beam line.

Track-based alignment techniques using cosmic muons were also applied to align the DT muon detectors in the barrel region of the experiment. An alignment precision of better than 700 μm was achieved along the higher precision coordinate direction (approximately ϕ) for the first three DT stations as estimated by a cross-check of extrapolating muon segments from one detector to the next [23]. A local alignment precision of 270 μm was achieved within each ring of CSCs using LHC beam-halo muons recorded during beam operations in 2008.

Studies of the resolution and efficiency of hit reconstruction in the DT [24] and CSC [19] muon chambers were performed. The resolution of a single reconstructed hit in a DT layer is of the order of 300 μm , and the efficiency of reconstructing high quality local track segments built from several layers in the DT chambers is approximately 99%. Likewise, the position resolution of local track segments in a CSC is of the order of 200 μm (50 μm for the highest $|\eta|$ chambers on $\text{YE}\pm 1$). The performance of the muon track reconstruction algorithms on CRAFT data was studied [25] using the muon system alone and using the muon system combined with the inner tracker. The requirement on the distance of closest approach to the beam line must be relaxed relative to that used for muons from collisions. The resolution of the track parameters can be determined by splitting a single cosmic ray signal into upper and lower tracks and comparing the results of the separate fits. For example, the p_{T} resolution for tracks passing close to the beam line with a sufficient number of hits in the silicon pixel and strip tracking detectors is measured to be of the order of 1% for $p_{\text{T}} = 10 \text{ GeV}/c$, increasing to 8% for p_{T} of about 500 GeV/c . The latter is limited by the accuracy of the alignment of the inner tracker and the muon system, and should improve to 5% when perfectly aligned.

Measurements of the cosmic muon energy loss, dE/dx , in the ECAL and HCAL barrel compartments validated the initial calibration of individual channels obtained prior to CRAFT (the endcap studies suffer from small sample sizes). In a study of 40% of the ECAL barrel channels, the obtained spread in detector response has an RMS of about 1.1%, consistent with the combined statistical and systematic uncertainties [15]. Additionally, the measured dE/dx as a function of muon momentum agrees well with a first-principles calculation [26]. For the HCAL barrel and endcap, CRAFT confirmed the brightening of scintillators with magnetic field first measured during MTCC, which leads to about a 9% increase in response. The response to cosmic muons recorded during CRAFT was used to adjust the intercalibration constants of the barrel, and the residual RMS spread is at the level of a few percent [16]. The absolute response to cosmic muons with a momentum of 150 GeV/c agrees well with earlier test beam measurements.

The accuracy of the calculated magnetic field map in the barrel steel yoke, used in muon reconstruction, was obtained by a comparison of the muon bending measured by DT chambers with the bending predicted by extrapolating the track parameters measured by the inner tracking system (where the magnetic field is known very precisely). During CRAFT a discrepancy was noted, and this was later traced to boundary conditions that had been set too restrictively in the field map calculation. The analysis also suggested improving the treatment of asymmetric features in the map. An updated field map was produced based on these results. Residual

differences between data and the calculation are reduced to about 4.5% in the middle station of the barrel yoke and 8.5% in the outer station, and are corrected using the CRAFT measurements [27].

7 Summary

The CRAFT exercise in 2008 provided invaluable experience in commissioning and operating the CMS experiment and, from analyses performed on the data recorded, in understanding the performance of its detectors. It represented a milestone in a global commissioning programme marked by a series of global data-taking periods with progressively larger fractions of the installed detectors participating, culminating in all installed systems read out in their entirety or nearly so. Over the course of 23 days during October and November 2008, the experiment collected 270 million cosmic ray triggered events with the solenoid at its operating central field of 3.8 T and with at least the silicon strip tracker and drift tube muon system participating and operating at nominal conditions. These data were processed by the offline data handling system, and then analyzed by teams dedicated to the calibration, alignment, and characterization of the detector subsystems. The precision achieved of detector calibrations and alignments, as well as operational experience of running the experiment for an extended period of time, give confidence that the CMS experiment is ready for LHC beam operations.

Acknowledgments

We thank the technical and administrative staff at CERN and other CMS Institutes, and acknowledge support from: FMSR (Austria); FNRS and FWO (Belgium); CNPq, CAPES, FAPERJ, and FAPESP (Brazil); MES (Bulgaria); CERN; CAS, MoST, and NSFC (China); COLCIENCIAS (Colombia); MSES (Croatia); RPF (Cyprus); Academy of Sciences and NICPB (Estonia); Academy of Finland, ME, and HIP (Finland); CEA and CNRS/IN2P3 (France); BMBF, DFG, and HGF (Germany); GSRT (Greece); OTKA and NKTH (Hungary); DAE and DST (India); IPM (Iran); SFI (Ireland); INFN (Italy); NRF (Korea); LAS (Lithuania); CINVESTAV, CONACYT, SEP, and UASLP-FAI (Mexico); PAEC (Pakistan); SCSR (Poland); FCT (Portugal); JINR (Armenia, Belarus, Georgia, Ukraine, Uzbekistan); MST and MAE (Russia); MSTDS (Serbia); MICINN and CPAN (Spain); Swiss Funding Agencies (Switzerland); NSC (Taipei); TUBITAK and TAEK (Turkey); STFC (United Kingdom); DOE and NSF (USA). Individuals have received support from the Marie-Curie IEF program (European Union); the Leventis Foundation; the A. P. Sloan Foundation; and the Alexander von Humboldt Foundation.

References

- [1] CMS Collaboration, "The CMS experiment at the CERN LHC", *JINST* **3** (2008) S08004. doi:10.1088/1748-0221/3/08/S08004.
- [2] L. Evans and P. Bryant (eds.), "LHC Machine", *JINST* **3** (2008) S08001. doi:10.1088/1748-0221/3/08/S08001.
- [3] A.J. Bell, "Beam & Radiation Monitoring for CMS", in *Nuclear Science Symposium Conference Record, 2008. NSS '08. IEEE*, pp. 2322–2325. Oct., 2008.
- [4] W. Lohmann et al., "Fast Beam Conditions Monitor BCM1F for the CMS Experiment", *accepted by Nucl. Instrum. Meth. A* (2009).

-
- [5] L. Agostino et al., “Commissioning of the CMS High Level Trigger”, *JINST* **4** (2009) P10005. doi:10.1088/1748-0221/4/10/P10005.
- [6] L.A. García-Moral et al., “Motions of CMS detector structures due to the magnetic field forces as observed by the Link alignment system during the test of the 4 T magnet solenoid”, *Nucl. Instrum. Meth.* **A606** (2009) 344. doi:10.1016/j.nima.2009.03.252.
- [7] V.I. Klyukhin et al., “Measurement of the CMS Magnetic Field”, *IEEE Transactions on Applied Superconductivity* **18** (2008) 395–398. doi:10.1109/TASC.2008.921242.
- [8] CMS Collaboration, “CMS Data Processing Workflows during an Extended Cosmic Ray Run”, *submitted to JINST* (2009).
- [9] CMS Collaboration, “Time Reconstruction and Performance of the CMS Electromagnetic Calorimeter”, *submitted to JINST* (2009).
- [10] CMS Collaboration, “Performance of CMS Hadron Calorimeter Timing and Synchronization using Cosmic Ray and LHC Beam Data”, *submitted to JINST* (2009).
- [11] CMS Collaboration, “Performance of the CMS Level-1 Trigger during Commissioning with Cosmic Rays”, *submitted to JINST* (2009).
- [12] CMS Collaboration, “Commissioning of the CMS High-Level Trigger with Cosmic Rays”, *submitted to JINST* (2009).
- [13] CMS Collaboration, “Performance and Operation of the CMS Silicon Strip Tracker with Cosmic Muons”, *submitted to JINST* (2009).
- [14] CMS Collaboration, “Commissioning and Performance of the CMS Pixel Tracker with Cosmic Rays”, *submitted to JINST* (2009).
- [15] CMS Collaboration, “Performance and Operation of the CMS Electromagnetic Calorimeter”, *submitted to JINST* (2009).
- [16] CMS Collaboration, “Performance of the CMS Hadron Calorimeter with Cosmic Ray and Accelerator Produced Muons”, *submitted to JINST* (2009).
- [17] CMS Collaboration, “Performance of the CMS Drift-Tube Chambers Local Trigger with Cosmic Rays”, *submitted to JINST* (2009).
- [18] CMS Collaboration, “Performance Study of the CMS Barrel Resistive Plate Chambers with Cosmic Rays”, *submitted to JINST* (2009).
- [19] CMS Collaboration, “Performance of the CMS Cathode Strip Chambers with Cosmic Rays”, *submitted to JINST* (2009).
- [20] L. Jones et al., “The APV25 deep submicron readout chip for CMS channels detectors”, *Proceedings of 5th workshop on Chips electronics for LHC experiments CERN/LHCC/99-09* (1999) 162–166.
- [21] CMS Collaboration, “Aligning the CMS Muon Chambers with the Muon Alignment System during an Extended Cosmic Ray Run”, *submitted to JINST* (2009).
- [22] CMS Collaboration, “Alignment of the CMS Silicon Tracker during Commissioning with Cosmic Rays”, *submitted to JINST* (2009).

- [23] CMS Collaboration, "Alignment of the CMS Muon System with Cosmic-Ray and Beam-Halo Muons", *submitted to JINST* (2009).
- [24] CMS Collaboration, "Performance of the CMS Drift Tube Chambers with Cosmic Rays", *submitted to JINST* (2009).
- [25] CMS Collaboration, "Performance of CMS Muon Reconstruction in Cosmic-Ray Events", *submitted to JINST* (2009).
- [26] CMS Collaboration, "Measurement of the Muon Stopping Power in Lead Tungstate", *submitted to JINST* (2009).
- [27] CMS Collaboration, "Precise Mapping of the Magnetic Field in the CMS Barrel Yoke using Cosmic Rays", *submitted to JINST* (2009).

A The CMS Collaboration

Yerevan Physics Institute, Yerevan, Armenia

S. Chatrchyan, V. Khachatryan, A.M. Sirunyan

Institut für Hochenergiephysik der OeAW, Wien, Austria

W. Adam, B. Arnold, H. Bergauer, T. Bergauer, M. Dragicevic, M. Eichberger, J. Erö, M. Friedl, R. Frühwirth, V.M. Ghete, J. Hammer¹, S. Hänsel, M. Hoch, N. Hörmann, J. Hrubec, M. Jeitler, G. Kasieczka, K. Kastner, M. Krammer, D. Liko, I. Magrans de Abril, I. Mikulec, F. Mittermayr, B. Neuherz, M. Oberegger, M. Padrta, M. Pernicka, H. Rohringer, S. Schmid, R. Schöfbeck, T. Schreiner, R. Stark, H. Steininger, J. Strauss, A. Taurok, F. Teischinger, T. Themel, D. Uhl, P. Wagner, W. Waltenberger, G. Walzel, E. Widl, C.-E. Wulz

National Centre for Particle and High Energy Physics, Minsk, Belarus

V. Chekhovsky, O. Dvornikov, I. Emelianchik, A. Litomin, V. Makarenko, I. Marfin, V. Mossolov, N. Shumeiko, A. Solin, R. Stefanovitch, J. Suarez Gonzalez, A. Tikhonov

Research Institute for Nuclear Problems, Minsk, Belarus

A. Fedorov, A. Karneyeu, M. Korzhik, V. Panov, R. Zuyevski

Research Institute of Applied Physical Problems, Minsk, Belarus

P. Kuchinsky

Universiteit Antwerpen, Antwerpen, Belgium

W. Beaumont, L. Benucci, M. Cardaci, E.A. De Wolf, E. Delmeire, D. Druzhkin, M. Hashemi, X. Janssen, T. Maes, L. Mucibello, S. Ochesanu, R. Rougny, M. Selvaggi, H. Van Haevermaet, P. Van Mechelen, N. Van Remortel

Vrije Universiteit Brussel, Brussel, Belgium

V. Adler, S. Beauceron, S. Blyweert, J. D'Hondt, S. De Weirdt, O. Devroede, J. Heyninck, A. Kalogeropoulos, J. Maes, M. Maes, M.U. Mozer, S. Tavernier, W. Van Doninck¹, P. Van Mulders, I. Villella

Université Libre de Bruxelles, Bruxelles, Belgium

O. Bouhali, E.C. Chabert, O. Charaf, B. Clerboux, G. De Lentdecker, V. Dero, S. Elgammal, A.P.R. Gay, G.H. Hammad, P.E. Marage, S. Rugovac, C. Vander Velde, P. Vanlaer, J. Wickens

Ghent University, Ghent, Belgium

M. Grunewald, B. Klein, A. Marinov, D. Ryckbosch, F. Thyssen, M. Tytgat, L. Vanelderen, P. Verwilligen

Université Catholique de Louvain, Louvain-la-Neuve, Belgium

S. Basesmez, G. Bruno, J. Caudron, C. Delaere, P. Demin, D. Favart, A. Giammanco, G. Grégoire, V. Lemaître, O. Militaru, S. Oryn, K. Piotrkowski¹, L. Quertenmont, N. Schul

Université de Mons, Mons, Belgium

N. Bely, E. Daubie

Centro Brasileiro de Pesquisas Fisicas, Rio de Janeiro, Brazil

G.A. Alves, M.E. Pol, M.H.G. Souza

Universidade do Estado do Rio de Janeiro, Rio de Janeiro, Brazil

W. Carvalho, D. De Jesus Damiao, C. De Oliveira Martins, S. Fonseca De Souza, L. Mundim, V. Oguri, A. Santoro, S.M. Silva Do Amaral, A. Sznajder

Instituto de Fisica Teorica, Universidade Estadual Paulista, Sao Paulo, Brazil

T.R. Fernandez Perez Tomei, M.A. Ferreira Dias, E. M. Gregores², S.F. Novaes

Institute for Nuclear Research and Nuclear Energy, Sofia, Bulgaria

K. Abadjiev¹, T. Anguelov, J. Damgov, N. Darmanov¹, L. Dimitrov, V. Genchev¹, P. Iaydjiev, S. Piperov, S. Stoykova, G. Sultanov, R. Trayanov, I. Vankov

University of Sofia, Sofia, Bulgaria

A. Dimitrov, M. Dyulendarova, V. Kozhuharov, L. Litov, E. Marinova, M. Mateev, B. Pavlov, P. Petkov, Z. Toteva¹

Institute of High Energy Physics, Beijing, China

G.M. Chen, H.S. Chen, W. Guan, C.H. Jiang, D. Liang, B. Liu, X. Meng, J. Tao, J. Wang, Z. Wang, Z. Xue, Z. Zhang

State Key Lab. of Nucl. Phys. and Tech., Peking University, Beijing, China

Y. Ban, J. Cai, Y. Ge, S. Guo, Z. Hu, Y. Mao, S.J. Qian, H. Teng, B. Zhu

Universidad de Los Andes, Bogota, Colombia

C. Avila, M. Baquero Ruiz, C.A. Carrillo Montoya, A. Gomez, B. Gomez Moreno, A.A. Ocampo Rios, A.F. Osorio Oliveros, D. Reyes Romero, J.C. Sanabria

Technical University of Split, Split, Croatia

N. Godinovic, K. Lelas, R. Plestina, D. Polic, I. Puljak

University of Split, Split, Croatia

Z. Antunovic, M. Dzelalija

Institute Rudjer Boskovic, Zagreb, Croatia

V. Brigljevic, S. Duric, K. Kadija, S. Morovic

University of Cyprus, Nicosia, Cyprus

R. Fereos, M. Galanti, J. Mousa, A. Papadakis, F. Ptochos, P.A. Razis, D. Tsiakkouri, Z. Zinonos

National Institute of Chemical Physics and Biophysics, Tallinn, Estonia

A. Hektor, M. Kadastik, K. Kannike, M. Müntel, M. Raidal, L. Rebane

Helsinki Institute of Physics, Helsinki, Finland

E. Anttila, S. Czellar, J. Härkönen, A. Heikkinen, V. Karimäki, R. Kinnunen, J. Klem, M.J. Kortelainen, T. Lampén, K. Lassila-Perini, S. Lehti, T. Lindén, P. Luukka, T. Mäenpää, J. Nysten, E. Tuominen, J. Tuominiemi, D. Ungaro, L. Wendland

Lappeenranta University of Technology, Lappeenranta, Finland

K. Banzuzi, A. Korpela, T. Tuuva

Laboratoire d'Annecy-le-Vieux de Physique des Particules, IN2P3-CNRS, Annecy-le-Vieux, France

P. Nedelec, D. Sillou

DSM/IRFU, CEA/Saclay, Gif-sur-Yvette, France

M. Besancon, R. Chipaux, M. Dejardin, D. Denegri, J. Descamps, B. Fabbro, J.L. Faure, F. Ferri, S. Ganjour, F.X. Gentit, A. Givernaud, P. Gras, G. Hamel de Monchenault, P. Jarry, M.C. Lemaire, E. Locci, J. Malcles, M. Marionneau, L. Millischer, J. Rander, A. Rosowsky, D. Rousseau, M. Titov, P. Verrecchia

Laboratoire Leprince-Ringuet, Ecole Polytechnique, IN2P3-CNRS, Palaiseau, France

S. Baffioni, L. Bianchini, M. Bluj³, P. Busson, C. Charlot, L. Dobrzynski, R. Granier de Cassagnac, M. Haguenaue, P. Miné, P. Paganini, Y. Sirois, C. Thiebaux, A. Zabi

Institut Pluridisciplinaire Hubert Curien, Université de Strasbourg, Université de Haute Alsace Mulhouse, CNRS/IN2P3, Strasbourg, France

J.-L. Agram⁴, A. Besson, D. Bloch, D. Bodin, J.-M. Brom, E. Conte⁴, F. Drouhin⁴, J.-C. Fontaine⁴, D. Gelé, U. Goerlach, L. Gross, P. Juillot, A.-C. Le Bihan, Y. Patois, J. Speck, P. Van Hove

Université de Lyon, Université Claude Bernard Lyon 1, CNRS-IN2P3, Institut de Physique Nucléaire de Lyon, Villeurbanne, France

C. Baty, M. Bedjidian, J. Blaha, G. Boudoul, H. Brun, N. Chanon, R. Chierici, D. Contardo, P. Depasse, T. Dupasquier, H. El Mamouni, F. Fassi⁵, J. Fay, S. Gascon, B. Ille, T. Kurca, T. Le Grand, M. Lethuillier, N. Lumb, L. Mirabito, S. Perries, M. Vander Donckt, P. Verdier

E. Andronikashvili Institute of Physics, Academy of Science, Tbilisi, Georgia

N. Djaoshvili, N. Roinishvili, V. Roinishvili

Institute of High Energy Physics and Informatization, Tbilisi State University, Tbilisi, Georgia

N. Amaglobeli

RWTH Aachen University, I. Physikalisches Institut, Aachen, Germany

R. Adolphi, G. Anagnostou, R. Brauer, W. Braunschweig, M. Edelhoff, H. Esser, L. Feld, W. Karpinski, A. Khomich, K. Klein, N. Mohr, A. Ostaptchouk, D. Pandoulas, G. Pierschel, F. Raupach, S. Schael, A. Schultz von Dratzig, G. Schwering, D. Sprenger, M. Thomas, M. Weber, B. Wittmer, M. Wlochal

RWTH Aachen University, III. Physikalisches Institut A, Aachen, Germany

O. Actis, G. Altenhöfer, W. Bender, P. Biallass, M. Erdmann, G. Fetchenhauer¹, J. Frangenheim, T. Hebbeker, G. Hilgers, A. Hinzmann, K. Hoepfner, C. Hof, M. Kirsch, T. Klimkovich, P. Kreuzer¹, D. Lanske[†], M. Merschmeyer, A. Meyer, B. Philipps, H. Pieta, H. Reithler, S.A. Schmitz, L. Sonnenschein, M. Sowa, J. Steggemann, H. Szczesny, D. Teyssier, C. Zeidler

RWTH Aachen University, III. Physikalisches Institut B, Aachen, Germany

M. Bontenackels, M. Davids, M. Duda, G. Flügge, H. Geenen, M. Giffels, W. Haj Ahmad, T. Hermanns, D. Heydhausen, S. Kalinin, T. Kress, A. Linn, A. Nowack, L. Perchalla, M. Poettgens, O. Pooth, P. Sauerland, A. Stahl, D. Tornier, M.H. Zoeller

Deutsches Elektronen-Synchrotron, Hamburg, Germany

M. Aldaya Martin, U. Behrens, K. Borrás, A. Campbell, E. Castro, D. Dammann, G. Eckerlin, A. Flossdorf, G. Flucke, A. Geiser, D. Hatton, J. Hauk, H. Jung, M. Kasemann, I. Katkov, C. Kleinwort, H. Kluge, A. Knutsson, E. Kuznetsova, W. Lange, W. Lohmann, R. Mankel¹, M. Marienfeld, A.B. Meyer, S. Miglioranza, J. Mnich, M. Ohlerich, J. Olzem, A. Parenti, C. Rosemann, R. Schmidt, T. Schoerner-Sadenius, D. Volynskyy, C. Wissing, W.D. Zeuner¹

University of Hamburg, Hamburg, Germany

C. Autermann, F. Bechtel, J. Draeger, D. Eckstein, U. Gebbert, K. Kaschube, G. Kaussen, R. Klanner, B. Mura, S. Naumann-Emme, F. Nowak, U. Pein, C. Sander, P. Schlexer, T. Schum, H. Stadie, G. Steinbrück, J. Thomsen, R. Wolf

Institut für Experimentelle Kernphysik, Karlsruhe, Germany

J. Bauer, P. Blüm, V. Buege, A. Cakir, T. Chwalek, W. De Boer, A. Dierlamm, G. Dirkes, M. Feindt, U. Felzmann, M. Frey, A. Furgeri, J. Gruschke, C. Hackstein, F. Hartmann¹, S. Heier, M. Heinrich, H. Held, D. Hirschbuehl, K.H. Hoffmann, S. Honc, C. Jung, T. Kuhr, T. Liamsuwan, D. Martschei, S. Mueller, Th. Müller, M.B. Neuland, M. Niegel, O. Oberst, A. Oehler, J. Ott, T. Peiffer, D. Piparo, G. Quast, K. Rabbertz, F. Ratnikov, N. Ratnikova, M. Renz, C. Saout¹, G. Sartisoehn, A. Scheurer, P. Schieferdecker, F.-P. Schilling, G. Schott, H.J. Simonis,

F.M. Stober, P. Sturm, D. Troendle, A. Trunov, W. Wagner, J. Wagner-Kuhr, M. Zeise, V. Zhukov⁶, E.B. Ziebarth

Institute of Nuclear Physics "Demokritos", Aghia Paraskevi, Greece

G. Daskalakis, T. Geralis, K. Karafasoulis, A. Kyriakis, D. Loukas, A. Markou, C. Markou, C. Mavrommatis, E. Petrakou, A. Zachariadou

University of Athens, Athens, Greece

L. Gouskos, P. Katsas, A. Panagiotou¹

University of Ioánnina, Ioánnina, Greece

I. Evangelou, P. Kokkas, N. Manthos, I. Papadopoulos, V. Patras, F.A. Triantis

KFKI Research Institute for Particle and Nuclear Physics, Budapest, Hungary

G. Bencze¹, L. Boldizsar, G. Debreczeni, C. Hajdu¹, S. Hernath, P. Hidas, D. Horvath⁷, K. Krajczar, A. Laszlo, G. Patay, F. Sikler, N. Toth, G. Vesztergombi

Institute of Nuclear Research ATOMKI, Debrecen, Hungary

N. Beni, G. Christian, J. Imrek, J. Molnar, D. Novak, J. Palinkas, G. Szekely, Z. Szillasi¹, K. Tokesi, V. Veszpremi

University of Debrecen, Debrecen, Hungary

A. Kapusi, G. Marian, P. Raics, Z. Szabo, Z.L. Trocsanyi, B. Ujvari, G. Zilizi

Panjab University, Chandigarh, India

S. Bansal, H.S. Bawa, S.B. Beri, V. Bhatnagar, M. Jindal, M. Kaur, R. Kaur, J.M. Kohli, M.Z. Mehta, N. Nishu, L.K. Saini, A. Sharma, A. Singh, J.B. Singh, S.P. Singh

University of Delhi, Delhi, India

S. Ahuja, S. Arora, S. Bhattacharya⁸, S. Chauhan, B.C. Choudhary, P. Gupta, S. Jain, S. Jain, M. Jha, A. Kumar, K. Ranjan, R.K. Shivpuri, A.K. Srivastava

Bhabha Atomic Research Centre, Mumbai, India

R.K. Choudhury, D. Dutta, S. Kailas, S.K. Kataria, A.K. Mohanty, L.M. Pant, P. Shukla, A. Topkar

Tata Institute of Fundamental Research - EHEP, Mumbai, India

T. Aziz, M. Guchait⁹, A. Gurtu, M. Maity¹⁰, D. Majumder, G. Majumder, K. Mazumdar, A. Nayak, A. Saha, K. Sudhakar

Tata Institute of Fundamental Research - HECR, Mumbai, India

S. Banerjee, S. Dugad, N.K. Mondal

Institute for Studies in Theoretical Physics & Mathematics (IPM), Tehran, Iran

H. Arfaei, H. Bakhshiansohi, A. Fahim, A. Jafari, M. Mohammadi Najafabadi, A. Moshaii, S. Paktinat Mehdiabadi, S. Rouhani, B. Safarzadeh, M. Zeinali

University College Dublin, Dublin, Ireland

M. Felcini

INFN Sezione di Bari ^a, Università di Bari ^b, Politecnico di Bari ^c, Bari, Italy

M. Abbrescia^{a,b}, L. Barbone^a, F. Chiumarulo^a, A. Clemente^a, A. Colaleo^a, D. Creanza^{a,c}, G. Cuscela^a, N. De Filippis^a, M. De Palma^{a,b}, G. De Robertis^a, G. Donvito^a, F. Fedele^a, L. Fiore^a, M. Franco^a, G. Iaselli^{a,c}, N. Lacalamita^a, F. Loddo^a, L. Lusito^{a,b}, G. Maggi^{a,c}, M. Maggi^a, N. Manna^{a,b}, B. Marangelli^{a,b}, S. My^{a,c}, S. Natali^{a,b}, S. Nuzzo^{a,b}, G. Papagni^a, S. Piccolomo^a, G.A. Pierro^a, C. Pinto^a, A. Pompili^{a,b}, G. Pugliese^{a,c}, R. Rajan^a, A. Ranieri^a, F. Romano^{a,c},

G. Roselli^{a,b}, G. Selvaggi^{a,b}, Y. Shinde^a, L. Silvestris^a, S. Tupputi^{a,b}, G. Zito^a

INFN Sezione di Bologna^a, Università di Bologna^b, Bologna, Italy

G. Abbiendi^a, W. Bacchi^{a,b}, A.C. Benvenuti^a, M. Boldini^a, D. Bonacorsi^a, S. Braibant-Giacomelli^{a,b}, V.D. Cafaro^a, S.S. Caiazza^a, P. Capiluppi^{a,b}, A. Castro^{a,b}, F.R. Cavallo^a, G. Codispoti^{a,b}, M. Cuffiani^{a,b}, I. D'Antone^a, G.M. Dallavalle^{a,1}, F. Fabbri^a, A. Fanfani^{a,b}, D. Fasanella^a, P. Giacomelli^a, V. Giordano^a, M. Giunta^{a,1}, C. Grandi^a, M. Guerzoni^a, S. Marcellini^a, G. Masetti^{a,b}, A. Montanari^a, F.L. Navarra^{a,b}, F. Odorici^a, G. Pellegrini^a, A. Perrotta^a, A.M. Rossi^{a,b}, T. Rovelli^{a,b}, G. Siroli^{a,b}, G. Torromeo^a, R. Travaglini^{a,b}

INFN Sezione di Catania^a, Università di Catania^b, Catania, Italy

S. Albergo^{a,b}, S. Costa^{a,b}, R. Potenza^{a,b}, A. Tricomi^{a,b}, C. Tuve^a

INFN Sezione di Firenze^a, Università di Firenze^b, Firenze, Italy

G. Barbagli^a, G. Broccolo^{a,b}, V. Ciulli^{a,b}, C. Civinini^a, R. D'Alessandro^{a,b}, E. Focardi^{a,b}, S. Frosali^{a,b}, E. Gallo^a, C. Genta^{a,b}, G. Landi^{a,b}, P. Lenzi^{a,b,1}, M. Meschini^a, S. Paoletti^a, G. Sguazzoni^a, A. Tropiano^a

INFN Laboratori Nazionali di Frascati, Frascati, Italy

L. Benussi, M. Bertani, S. Bianco, S. Colafranceschi¹¹, D. Colonna¹¹, F. Fabbri, M. Giardoni, L. Passamonti, D. Piccolo, D. Pierluigi, B. Ponzio, A. Russo

INFN Sezione di Genova, Genova, Italy

P. Fabbriatore, R. Musenich

INFN Sezione di Milano-Bicocca^a, Università di Milano-Bicocca^b, Milano, Italy

A. Benaglia^a, M. Calloni^a, G.B. Cerati^{a,b,1}, P. D'Angelo^a, F. De Guio^a, F.M. Farina^a, A. Ghezzi^a, P. Govoni^{a,b}, M. Malberti^{a,b,1}, S. Malvezzi^a, A. Martelli^a, D. Menasce^a, V. Miccio^{a,b}, L. Moroni^a, P. Negri^{a,b}, M. Paganoni^{a,b}, D. Pedrini^a, A. Pullia^{a,b}, S. Ragazzi^{a,b}, N. Redaelli^a, S. Sala^a, R. Salerno^{a,b}, T. Tabarelli de Fatis^{a,b}, V. Tancini^{a,b}, S. Taroni^{a,b}

INFN Sezione di Napoli^a, Università di Napoli "Federico II"^b, Napoli, Italy

S. Buontempo^a, N. Cavallo^a, A. Cimmino^{a,b,1}, M. De Gruttola^{a,b,1}, F. Fabozzi^{a,12}, A.O.M. Iorio^a, L. Lista^a, D. Lomidze^a, P. Noli^{a,b}, P. Paolucci^a, C. Sciacca^{a,b}

INFN Sezione di Padova^a, Università di Padova^b, Padova, Italy

P. Azzi^{a,1}, N. Bacchetta^a, L. Barcellan^a, P. Bellan^{a,b,1}, M. Bellato^a, M. Benettoni^a, M. Biasotto^{a,13}, D. Bisello^{a,b}, E. Borsato^{a,b}, A. Branca^a, R. Carlin^{a,b}, L. Castellani^a, P. Checchia^a, E. Conti^a, F. Dal Corso^a, M. De Mattia^{a,b}, T. Dorigo^a, U. Dosselli^a, F. Fanzago^a, F. Gasparini^{a,b}, U. Gasparini^{a,b}, P. Giubileo^{a,b}, F. Gonella^a, A. Gresele^{a,14}, M. Gulmini^{a,13}, A. Kaminskiy^{a,b}, S. Lacaprara^{a,13}, I. Lazzizzera^{a,14}, M. Margoni^{a,b}, G. Maron^{a,13}, S. Mattiazzo^{a,b}, M. Mazzucato^a, M. Meneghelli^a, A.T. Meneguzzo^{a,b}, M. Michelotto^a, F. Montecassiano^a, M. Nespolo^a, M. Passaseo^a, M. Pegoraro^a, L. Perrozzi^a, N. Pozzobon^{a,b}, P. Ronchese^{a,b}, F. Simonetto^{a,b}, N. Toniolo^a, E. Torassa^a, M. Tosi^{a,b}, A. Triossi^a, S. Vanini^{a,b}, S. Ventura^a, P. Zotto^{a,b}, G. Zumerle^{a,b}

INFN Sezione di Pavia^a, Università di Pavia^b, Pavia, Italy

P. Baesso^{a,b}, U. Berzano^a, S. Bricola^a, M.M. Necchi^{a,b}, D. Pagano^{a,b}, S.P. Ratti^{a,b}, C. Riccardi^{a,b}, P. Torre^{a,b}, A. Vicini^a, P. Vitulo^{a,b}, C. Viviani^{a,b}

INFN Sezione di Perugia^a, Università di Perugia^b, Perugia, Italy

D. Aisa^a, S. Aisa^a, E. Babucci^a, M. Biasini^{a,b}, G.M. Bilei^a, B. Caponeri^{a,b}, B. Checcucci^a, N. Dinu^a, L. Fanò^a, L. Farnesini^a, P. Lariccia^{a,b}, A. Lucaroni^{a,b}, G. Mantovani^{a,b}, A. Nappi^{a,b}, A. Piluso^a, V. Postolache^a, A. Santocchia^{a,b}, L. Servoli^a, D. Tonoiu^a, A. Vedae^a, R. Volpe^{a,b}

INFN Sezione di Pisa ^a, Universita di Pisa ^b, Scuola Normale Superiore di Pisa ^c, Pisa, Italy
 P. Azzurri^{a,c}, G. Bagliesi^a, J. Bernardini^{a,b}, L. Berretta^a, T. Boccali^a, A. Bocci^{a,c}, L. Borrello^{a,c},
 F. Bosi^a, F. Calzolari^a, R. Castaldi^a, R. Dell’Orso^a, F. Fiori^{a,b}, L. Foà^{a,c}, S. Gennai^{a,c}, A. Giassi^a,
 A. Kraan^a, F. Ligabue^{a,c}, T. Lomtadze^a, F. Mariani^a, L. Martini^a, M. Massa^a, A. Messineo^{a,b},
 A. Moggi^a, F. Palla^a, F. Palmonari^a, G. Petraghani^a, G. Petrucciani^{a,c}, F. Raffaelli^a, S. Sarkar^a,
 G. Segneri^a, A.T. Serban^a, P. Spagnolo^{a,1}, R. Tenchini^{a,1}, S. Tolaini^a, G. Tonelli^{a,b,1}, A. Venturi^a,
 P.G. Verdini^a

INFN Sezione di Roma ^a, Universita di Roma “La Sapienza” ^b, Roma, Italy
 S. Baccaro^{a,15}, L. Barone^{a,b}, A. Bartoloni^a, F. Cavallari^{a,1}, I. Dafinei^a, D. Del Re^{a,b}, E. Di
 Marco^{a,b}, M. Diemoz^a, D. Franci^{a,b}, E. Longo^{a,b}, G. Organtini^{a,b}, A. Palma^{a,b}, F. Pandolfi^{a,b},
 R. Paramatti^{a,1}, F. Pellegrino^a, S. Rahatlou^{a,b}, C. Rovelli^a

**INFN Sezione di Torino ^a, Università di Torino ^b, Università del Piemonte Orientale (No-
 vara) ^c, Torino, Italy**
 G. Alampi^a, N. Amapane^{a,b}, R. Arcidiacono^{a,b}, S. Argiro^{a,b}, M. Arneodo^{a,c}, C. Biino^a,
 M.A. Borgia^{a,b}, C. Botta^{a,b}, N. Cartiglia^a, R. Castello^{a,b}, G. Cerminara^{a,b}, M. Costa^{a,b},
 D. Dattola^a, G. Dellacasa^a, N. Demaria^a, G. Dughera^a, F. Dumitrache^a, A. Graziano^{a,b},
 C. Mariotti^a, M. Marone^{a,b}, S. Maselli^a, E. Migliore^{a,b}, G. Mila^{a,b}, V. Monaco^{a,b}, M. Musich^{a,b},
 M. Nervo^{a,b}, M.M. Obertino^{a,c}, S. Oggero^{a,b}, R. Panero^a, N. Pastrone^a, M. Pelliccioni^{a,b},
 A. Romero^{a,b}, M. Ruspa^{a,c}, R. Sacchi^{a,b}, A. Solano^{a,b}, A. Staiano^a, P.P. Trapani^{a,b,1}, D. Trocino^{a,b},
 A. Vilela Pereira^{a,b}, L. Visca^{a,b}, A. Zampieri^a

INFN Sezione di Trieste ^a, Universita di Trieste ^b, Trieste, Italy
 F. Ambroglini^{a,b}, S. Belforte^a, F. Cossutti^a, G. Della Ricca^{a,b}, B. Gobbo^a, A. Penzo^a

Kyungpook National University, Daegu, Korea
 S. Chang, J. Chung, D.H. Kim, G.N. Kim, D.J. Kong, H. Park, D.C. Son

Wonkwang University, Iksan, Korea
 S.Y. Bahk

Chonnam National University, Kwangju, Korea
 S. Song

Konkuk University, Seoul, Korea
 S.Y. Jung

Korea University, Seoul, Korea
 B. Hong, H. Kim, J.H. Kim, K.S. Lee, D.H. Moon, S.K. Park, H.B. Rhee, K.S. Sim

Seoul National University, Seoul, Korea
 J. Kim

University of Seoul, Seoul, Korea
 M. Choi, G. Hahn, I.C. Park

Sungkyunkwan University, Suwon, Korea
 S. Choi, Y. Choi, J. Goh, H. Jeong, T.J. Kim, J. Lee, S. Lee

Vilnius University, Vilnius, Lithuania
 M. Janulis, D. Martisiute, P. Petrov, T. Sabonis

Centro de Investigacion y de Estudios Avanzados del IPN, Mexico City, Mexico
 H. Castilla Valdez¹, A. Sánchez Hernández

Universidad Iberoamericana, Mexico City, Mexico

S. Carrillo Moreno

Universidad Autónoma de San Luis Potosí, San Luis Potosí, Mexico

A. Morelos Pineda

University of Auckland, Auckland, New Zealand

P. Allfrey, R.N.C. Gray, D. Krofcheck

University of Canterbury, Christchurch, New Zealand

N. Bernardino Rodrigues, P.H. Butler, T. Signal, J.C. Williams

National Centre for Physics, Quaid-I-Azam University, Islamabad, Pakistan

M. Ahmad, I. Ahmed, W. Ahmed, M.I. Asghar, M.I.M. Awan, H.R. Hoorani, I. Hussain, W.A. Khan, T. Khurshid, S. Muhammad, S. Qazi, H. Shahzad

Institute of Experimental Physics, Warsaw, PolandM. Cwiok, R. Dabrowski, W. Dominik, K. Doroba, M. Konecki, J. Krolikowski, K. Pozniak¹⁶, R. Romaniuk, W. Zabolotny¹⁶, P. Zych**Soltan Institute for Nuclear Studies, Warsaw, Poland**

T. Frueboes, R. Gokieli, L. Gosciolo, M. Górski, M. Kazana, K. Nawrocki, M. Szleper, G. Wrochna, P. Zalewski

Laboratório de Instrumentação e Física Experimental de Partículas, Lisboa, Portugal

N. Almeida, L. Antunes Pedro, P. Bargassa, A. David, P. Faccioli, P.G. Ferreira Parracho, M. Freitas Ferreira, M. Gallinaro, M. Guerra Jordao, P. Martins, G. Mini, P. Musella, J. Pela, L. Raposo, P.Q. Ribeiro, S. Sampaio, J. Seixas, J. Silva, P. Silva, D. Soares, M. Sousa, J. Varela, H.K. Wöhri

Joint Institute for Nuclear Research, Dubna, Russia

I. Altsybeev, I. Belotelov, P. Bunin, Y. Ershov, I. Filozova, M. Finger, M. Finger Jr., A. Golunov, I. Golutvin, N. Gorbounov, V. Kalagin, A. Kamenev, V. Karjavin, V. Konoplyanikov, V. Korenkov, G. Kozlov, A. Kurenkov, A. Lanev, A. Makankin, V.V. Mitsyn, P. Moisezen, E. Nikonov, D. Oleynik, V. Palichik, V. Perelygin, A. Petrosyan, R. Semenov, S. Shmatov, V. Smirnov, D. Smolin, E. Tikhonenko, S. Vasil'ev, A. Vishnevskiy, A. Volodko, A. Zarubin, V. Zhiltsov

Petersburg Nuclear Physics Institute, Gatchina (St Petersburg), Russia

N. Bondar, L. Chtchipounov, A. Denisov, Y. Gavrikov, G. Gavrilo, V. Golovtsov, Y. Ivanov, V. Kim, V. Kozlov, P. Levchenko, G. Obrant, E. Orishchin, A. Petrunin, Y. Shcheglov, A. Shchetkovskiy, V. Sknar, I. Smirnov, V. Sulimov, V. Tarakanov, L. Uvarov, S. Vavilov, G. Velichko, S. Volkov, A. Vorobyev

Institute for Nuclear Research, Moscow, Russia

Yu. Andreev, A. Anisimov, P. Antipov, A. Dermenev, S. Gninenko, N. Golubev, M. Kirsanov, N. Krasnikov, V. Matveev, A. Pashenkov, V.E. Postoev, A. Solovey, A. Solovey, A. Toropin, S. Troitsky

Institute for Theoretical and Experimental Physics, Moscow, RussiaA. Baud, V. Epshteyn, V. Gavrilov, N. Ilina, V. Kaftanov[†], V. Kolosov, M. Kossov¹, A. Krokhotin, S. Kuleshov, A. Oulianov, G. Safronov, S. Semenov, I. Shreyber, V. Stolin, E. Vlasov, A. Zhokin**Moscow State University, Moscow, Russia**E. Boos, M. Dubinin¹⁷, L. Dudko, A. Ershov, A. Gribushin, V. Klyukhin, O. Kodolova, I. Lokhtin, S. Petrushanko, L. Sarycheva, V. Savrin, A. Snigirev, I. Vardanyan

P.N. Lebedev Physical Institute, Moscow, Russia

I. Dremin, M. Kirakosyan, N. Konovalova, S.V. Rusakov, A. Vinogradov

State Research Center of Russian Federation, Institute for High Energy Physics, Protvino, Russia

S. Akimenko, A. Artamonov, I. Azhgirey, S. Bitioukov, V. Burtovoy, V. Grishin¹, V. Kachanov, D. Konstantinov, V. Krychkin, A. Levine, I. Lobov, V. Lukanin, Y. Mel'nik, V. Petrov, R. Ryutin, S. Slabospitsky, A. Sobol, A. Sytine, L. Tourtchanovitch, S. Troshin, N. Tyurin, A. Uzunian, A. Volkov

Vinca Institute of Nuclear Sciences, Belgrade, Serbia

P. Adzic, M. Djordjevic, D. Jovanovic¹⁸, D. Krpic¹⁸, D. Maletic, J. Puzovic¹⁸, N. Smiljkovic

Centro de Investigaciones Energéticas Medioambientales y Tecnológicas (CIEMAT), Madrid, Spain

M. Aguilar-Benitez, J. Alberdi, J. Alcaraz Maestre, P. Arce, J.M. Barcala, C. Battilana, C. Burgos Lazaro, J. Caballero Bejar, E. Calvo, M. Cardenas Montes, M. Cepeda, M. Cerrada, M. Chamizo Llatas, F. Clemente, N. Colino, M. Daniel, B. De La Cruz, A. Delgado Peris, C. Diez Pardos, C. Fernandez Bedoya, J.P. Fernández Ramos, A. Ferrando, J. Flix, M.C. Fouz, P. Garcia-Abia, A.C. Garcia-Bonilla, O. Gonzalez Lopez, S. Goy Lopez, J.M. Hernandez, M.I. Josa, J. Marin, G. Merino, J. Molina, A. Molinero, J.J. Navarrete, J.C. Oller, J. Puerta Pelayo, L. Romero, J. Santaolalla, C. Villanueva Munoz, C. Willmott, C. Yuste

Universidad Autónoma de Madrid, Madrid, Spain

C. Albajar, M. Blanco Otano, J.F. de Trocóniz, A. Garcia Raboso, J.O. Lopez Berengueres

Universidad de Oviedo, Oviedo, Spain

J. Cuevas, J. Fernandez Menendez, I. Gonzalez Caballero, L. Lloret Iglesias, H. Naves Sordo, J.M. Vizan Garcia

Instituto de Física de Cantabria (IFCA), CSIC-Universidad de Cantabria, Santander, Spain

I.J. Cabrillo, A. Calderon, S.H. Chuang, I. Diaz Merino, C. Diez Gonzalez, J. Duarte Campderros, M. Fernandez, G. Gomez, J. Gonzalez Sanchez, R. Gonzalez Suarez, C. Jorda, P. Lobelle Pardo, A. Lopez Virto, J. Marco, R. Marco, C. Martinez Rivero, P. Martinez Ruiz del Arbol, F. Matorras, T. Rodrigo, A. Ruiz Jimeno, L. Scodellaro, M. Sobron Sanudo, I. Vila, R. Vilar Cortabitarte

CERN, European Organization for Nuclear Research, Geneva, Switzerland

D. Abbaneo, E. Albert, M. Alidra, S. Ashby, E. Auffray, J. Baechler, P. Baillon, A.H. Ball, S.L. Bally, D. Barney, F. Beaudette¹⁹, R. Bellan, D. Benedetti, G. Benelli, C. Bernet, P. Bloch, S. Bolognesi, M. Bona, J. Bos, N. Bourgeois, T. Bourrel, H. Breuker, K. Bunkowski, D. Campi, T. Camporesi, E. Cano, A. Cattai, J.P. Chatelain, M. Chauvey, T. Christiansen, J.A. Coarasa Perez, A. Conde Garcia, R. Covarelli, B. Curé, A. De Roeck, V. Delachenal, D. Deyrail, S. Di Vincenzo²⁰, S. Dos Santos, T. Dupont, L.M. Edera, A. Elliott-Peisert, M. Eppard, M. Favre, N. Frank, W. Funk, A. Gaddi, M. Gastal, M. Gateau, H. Gerwig, D. Gigi, K. Gill, D. Giordano, J.P. Girod, F. Glege, R. Gomez-Reino Garrido, R. Goudard, S. Gowdy, R. Guida, L. Guiducci, J. Gutleber, M. Hansen, C. Hartl, J. Harvey, B. Hegner, H.F. Hoffmann, A. Holzner, A. Honma, M. Huhtinen, V. Innocente, P. Janot, G. Le Godec, P. Lecoq, C. Leonidopoulos, R. Loos, C. Lourenço, A. Lyonnet, A. Macpherson, N. Magini, J.D. Maillefaud, G. Maire, T. Mäki, L. Malgeri, M. Mannelli, L. Masetti, F. Meijers, P. Meridiani, S. Mersi, E. Meschi, A. Meynet Cordonnier, R. Moser, M. Mulders, J. Mulon, M. Noy, A. Oh, G. Olesen, A. Onnela, T. Orimoto, L. Orsini, E. Perez, G. Perinic, J.F. Pernot, P. Petagna, P. Petiot, A. Petrilli, A. Pfeiffer, M. Pierini, M. Pimiä, R. Pintus, B. Pirollet, H. Postema, A. Racz, S. Ravat, S.B. Rew, J. Rodrigues Antunes,

G. Rolandi²¹, M. Rovere, V. Ryjov, H. Sakulin, D. Samyn, H. Sauce, C. Schäfer, W.D. Schlatter, M. Schröder, C. Schwick, A. Sciaba, I. Segoni, A. Sharma, N. Siegrist, P. Siegrist, N. Sinanis, T. Sobrier, P. Sphicas²², D. Spiga, M. Spiropulu¹⁷, F. Stöckli, P. Traczyk, P. Tropea, J. Troska, A. Tsirou, L. Veillet, G.I. Veres, M. Voutilainen, P. Wertelaers, M. Zanetti

Paul Scherrer Institut, Villigen, Switzerland

W. Bertl, K. Deiters, W. Erdmann, K. Gabathuler, R. Horisberger, Q. Ingram, H.C. Kaestli, S. König, D. Kotlinski, U. Langenegger, F. Meier, D. Renker, T. Rohe, J. Sibille²³, A. Starodumov²⁴

Institute for Particle Physics, ETH Zurich, Zurich, Switzerland

B. Betev, L. Caminada²⁵, Z. Chen, S. Cittolin, D.R. Da Silva Di Calafiori, S. Dambach²⁵, G. Dissertori, M. Dittmar, C. Eggel²⁵, J. Eugster, G. Faber, K. Freudenreich, C. Grab, A. Hervé, W. Hintz, P. Lecomte, P.D. Luckey, W. Lustermann, C. Marchica²⁵, P. Milenovic²⁶, F. Moortgat, A. Nardulli, F. Nessi-Tedaldi, L. Pape, F. Pauss, T. Punz, A. Rizzi, F.J. Ronga, L. Sala, A.K. Sanchez, M.-C. Sawley, V. Sordini, B. Stieger, L. Tauscher[†], A. Thea, K. Theofilatos, D. Treille, P. Trüb²⁵, M. Weber, L. Wehrli, J. Weng, S. Zelepoukine²⁷

Universität Zürich, Zurich, Switzerland

C. Amsler, V. Chiochia, S. De Visscher, C. Regenfus, P. Robmann, T. Rommerskirchen, A. Schmidt, D. Tsirigkas, L. Wilke

National Central University, Chung-Li, Taiwan

Y.H. Chang, E.A. Chen, W.T. Chen, A. Go, C.M. Kuo, S.W. Li, W. Lin

National Taiwan University (NTU), Taipei, Taiwan

P. Bartalini, P. Chang, Y. Chao, K.F. Chen, W.-S. Hou, Y. Hsiung, Y.J. Lei, S.W. Lin, R.-S. Lu, J. Schümann, J.G. Shiu, Y.M. Tzeng, K. Ueno, Y. Velikzhanin, C.C. Wang, M. Wang

Cukurova University, Adana, Turkey

A. Adiguzel, A. Ayhan, A. Azman Gokce, M.N. Bakirci, S. Cerci, I. Dumanoglu, E. Eskut, S. Girgis, E. Gurpinar, I. Hos, T. Karaman, T. Karaman, A. Kayis Topaksu, P. Kurt, G. Önengüt, G. Önengüt Gökbulut, K. Ozdemir, S. Ozturk, A. Polatöz, K. Sogut²⁸, B. Tali, H. Topakli, D. Uzun, L.N. Vergili, M. Vergili

Middle East Technical University, Physics Department, Ankara, Turkey

I.V. Akin, T. Aliev, S. Bilmis, M. Deniz, H. Gamsizkan, A.M. Guler, K. Öcalan, M. Serin, R. Sever, U.E. Surat, M. Zeyrek

Bogaziçi University, Department of Physics, Istanbul, Turkey

M. Deliomeroglu, D. Demir²⁹, E. Gülmez, A. Halu, B. Isildak, M. Kaya³⁰, O. Kaya³⁰, S. Ozkorucuklu³¹, N. Sonmez³²

National Scientific Center, Kharkov Institute of Physics and Technology, Kharkov, Ukraine

L. Levchuk, S. Lukyanenko, D. Soroka, S. Zub

University of Bristol, Bristol, United Kingdom

F. Bostock, J.J. Brooke, T.L. Cheng, D. Cussans, R. Frazier, J. Goldstein, N. Grant, M. Hansen, G.P. Heath, H.F. Heath, C. Hill, B. Huckvale, J. Jackson, C.K. Mackay, S. Metson, D.M. Newbold³³, K. Nirunpong, V.J. Smith, J. Velthuis, R. Walton

Rutherford Appleton Laboratory, Didcot, United Kingdom

K.W. Bell, C. Brew, R.M. Brown, B. Camanzi, D.J.A. Cockerill, J.A. Coughlan, N.I. Geddes, K. Harder, S. Harper, B.W. Kennedy, P. Murray, C.H. Shepherd-Themistocleous, I.R. Tomalin, J.H. Williams[†], W.J. Womersley, S.D. Worm

Imperial College, University of London, London, United Kingdom

R. Bainbridge, G. Ball, J. Ballin, R. Beuselinck, O. Buchmuller, D. Colling, N. Cripps, G. Davies, M. Della Negra, C. Foudas, J. Fulcher, D. Futyan, G. Hall, J. Hays, G. Iles, G. Karapostoli, B.C. MacEvoy, A.-M. Magnan, J. Marrouche, J. Nash, A. Nikitenko²⁴, A. Papageorgiou, M. Pesaresi, K. Petridis, M. Pioppi³⁴, D.M. Raymond, N. Rompotis, A. Rose, M.J. Ryan, C. Seez, P. Sharp, G. Sidiropoulos¹, M. Stettler, M. Stoye, M. Takahashi, A. Tapper, C. Timlin, S. Tourneur, M. Vazquez Acosta, T. Virdee¹, S. Wakefield, D. Wardrope, T. Whyntie, M. Wingham

Brunel University, Uxbridge, United Kingdom

J.E. Cole, I. Goitom, P.R. Hobson, A. Khan, P. Kyberd, D. Leslie, C. Munro, I.D. Reid, C. Siमितros, R. Taylor, L. Teodorescu, I. Yaselli

Boston University, Boston, USA

T. Bose, M. Carleton, E. Hazen, A.H. Heering, A. Heister, J. St. John, P. Lawson, D. Lazic, D. Osborne, J. Rohlf, L. Sulak, S. Wu

Brown University, Providence, USA

J. Andrea, A. Avetisyan, S. Bhattacharya, J.P. Chou, D. Cutts, S. Esen, G. Kukartsev, G. Landsberg, M. Narain, D. Nguyen, T. Speer, K.V. Tsang

University of California, Davis, Davis, USA

R. Breedon, M. Calderon De La Barca Sanchez, M. Case, D. Cebra, M. Chertok, J. Conway, P.T. Cox, J. Dolen, R. Erbacher, E. Friis, W. Ko, A. Kopecky, R. Lander, A. Lister, H. Liu, S. Maruyama, T. Miceli, M. Nikolic, D. Pellett, J. Robles, M. Searle, J. Smith, M. Squires, J. Stilley, M. Tripathi, R. Vasquez Sierra, C. Veelken

University of California, Los Angeles, Los Angeles, USA

V. Andreev, K. Arisaka, D. Cline, R. Cousins, S. Erhan¹, J. Hauser, M. Ignatenko, C. Jarvis, J. Mumford, C. Plager, G. Rakness, P. Schlein[†], J. Tucker, V. Valuev, R. Wallny, X. Yang

University of California, Riverside, Riverside, USA

J. Babb, M. Bose, A. Chandra, R. Clare, J.A. Ellison, J.W. Gary, G. Hanson, G.Y. Jeng, S.C. Kao, F. Liu, H. Liu, A. Luthra, H. Nguyen, G. Pasztor³⁵, A. Satpathy, B.C. Shen[†], R. Stringer, J. Sturdy, V. Sytnik, R. Wilken, S. Wimpenny

University of California, San Diego, La Jolla, USA

J.G. Branson, E. Dusinger, D. Evans, F. Golf, R. Kelley, M. Lebourgeois, J. Letts, E. Lipeles, B. Mangano, J. Muelmenstaedt, M. Norman, S. Padhi, A. Petrucci, H. Pi, M. Pieri, R. Ranieri, M. Sani, V. Sharma, S. Simon, F. Würthwein, A. Yagil

University of California, Santa Barbara, Santa Barbara, USA

C. Campagnari, M. D'Alfonso, T. Danielson, J. Garberson, J. Incandela, C. Justus, P. Kalavase, S.A. Koay, D. Kovalskyi, V. Krutelyov, J. Lamb, S. Lowette, V. Pavlunin, F. Rebassoo, J. Ribnik, J. Richman, R. Rossin, D. Stuart, W. To, J.R. Vlimant, M. Witherell

California Institute of Technology, Pasadena, USA

A. Apresyan, A. Bornheim, J. Bunn, M. Chiorboli, M. Gataullin, D. Kcira, V. Litvine, Y. Ma, H.B. Newman, C. Rogan, V. Timciuc, J. Veverka, R. Wilkinson, Y. Yang, L. Zhang, K. Zhu, R.Y. Zhu

Carnegie Mellon University, Pittsburgh, USA

B. Akgun, R. Carroll, T. Ferguson, D.W. Jang, S.Y. Jun, M. Paulini, J. Russ, N. Terentyev, H. Vogel, I. Vorobiev

University of Colorado at Boulder, Boulder, USA

J.P. Cumalat, M.E. Dinardo, B.R. Drell, W.T. Ford, B. Heyburn, E. Luiggi Lopez, U. Nauenberg, K. Stenson, K. Ulmer, S.R. Wagner, S.L. Zang

Cornell University, Ithaca, USA

L. Agostino, J. Alexander, F. Blekman, D. Cassel, A. Chatterjee, S. Das, L.K. Gibbons, B. Heltsley, W. Hopkins, A. Khukhunaishvili, B. Kreis, V. Kuznetsov, J.R. Patterson, D. Puigh, A. Ryd, X. Shi, S. Stroiney, W. Sun, W.D. Teo, J. Thom, J. Vaughan, Y. Weng, P. Wittich

Fairfield University, Fairfield, USA

C.P. Beetz, G. Cirino, C. Sanzeni, D. Winn

Fermi National Accelerator Laboratory, Batavia, USA

S. Abdullin, M.A. Afaq¹, M. Albrow, B. Ananthan, G. Apollinari, M. Atac, W. Badgett, L. Bagby, J.A. Bakken, B. Baldin, S. Banerjee, K. Banicz, L.A.T. Bauerdick, A. Beretvas, J. Berryhill, P.C. Bhat, K. Biery, M. Binkley, I. Bloch, F. Borcherding, A.M. Brett, K. Burkett, J.N. Butler, V. Chetluru, H.W.K. Cheung, F. Chlebana, I. Churin, S. Cihangir, M. Crawford, W. Dagenhart, M. Demarteau, G. Derylo, D. Dykstra, D.P. Eartly, J.E. Elias, V.D. Elvira, D. Evans, L. Feng, M. Fischler, I. Fisk, S. Foulkes, J. Freeman, P. Gartung, E. Gottschalk, T. Grassi, D. Green, Y. Guo, O. Gutsche, A. Hahn, J. Hanlon, R.M. Harris, B. Holzman, J. Howell, D. Hufnagel, E. James, H. Jensen, M. Johnson, C.D. Jones, U. Joshi, E. Juska, J. Kaiser, B. Klima, S. Kossiakov, K. Kousouris, S. Kwan, C.M. Lei, P. Limon, J.A. Lopez Perez, S. Los, L. Lueking, G. Lukhanin, S. Lusin¹, J. Lykken, K. Maeshima, J.M. Marraffino, D. Mason, P. McBride, T. Miao, K. Mishra, S. Moccia, R. Mommsen, S. Mrenna, A.S. Muhammad, C. Newman-Holmes, C. Noeding, V. O'Dell, O. Prokofyev, R. Rivera, C.H. Rivetta, A. Ronzhin, P. Rossman, S. Ryu, V. Sekhri, E. Sexton-Kennedy, I. Sfiligoi, S. Sharma, T.M. Shaw, D. Shpakov, E. Skup, R.P. Smith[†], A. Soha, W.J. Spalding, L. Spiegel, I. Suzuki, P. Tan, W. Tanenbaum, S. Tkaczyk¹, R. Trentadue¹, L. Up-
legger, E.W. Vaandering, R. Vidal, J. Whitmore, E. Wicklund, W. Wu, J. Yarba, F. Yumiceva, J.C. Yun

University of Florida, Gainesville, USA

D. Acosta, P. Avery, V. Barashko, D. Bourilkov, M. Chen, G.P. Di Giovanni, D. Dobur, A. Drozdetskiy, R.D. Field, Y. Fu, I.K. Furic, J. Gartner, D. Holmes, B. Kim, S. Klimentko, J. Konigsberg, A. Korytov, K. Kotov, A. Kropivnitskaya, T. Kypreos, A. Madorsky, K. Matchev, G. Mitselmakher, Y. Pakhotin, J. Piedra Gomez, C. Prescott, V. Rapsevicius, R. Remington, M. Schmitt, B. Scurlock, D. Wang, J. Yelton

Florida International University, Miami, USA

C. Ceron, V. Gaultney, L. Kramer, L.M. Lebolo, S. Linn, P. Markowitz, G. Martinez, J.L. Rodriguez

Florida State University, Tallahassee, USA

T. Adams, A. Askew, H. Baer, M. Bertoldi, J. Chen, W.G.D. Dharmaratna, S.V. Gleyzer, J. Haas, S. Hagopian, V. Hagopian, M. Jenkins, K.F. Johnson, E. Prettner, H. Prosper, S. Sekmen

Florida Institute of Technology, Melbourne, USA

M.M. Baarmand, S. Guragain, M. Hohmann, H. Kalakhety, H. Mermerkaya, R. Ralich, I. Vodopyanov

University of Illinois at Chicago (UIC), Chicago, USA

B. Abelev, M.R. Adams, I.M. Anghel, L. Apanasevich, V.E. Bazterra, R.R. Betts, J. Callner, M.A. Castro, R. Cavanaugh, C. Dragoiu, E.J. Garcia-Solis, C.E. Gerber, D.J. Hofman, S. Khalatian, C. Mironov, E. Shabalina, A. Smoron, N. Varelas

The University of Iowa, Iowa City, USA

U. Akgun, E.A. Albayrak, A.S. Ayan, B. Bilki, R. Briggs, K. Cankocak³⁶, K. Chung, W. Clarida, P. Debbins, F. Duru, F.D. Ingram, C.K. Lae, E. McCliment, J.-P. Merlo, A. Mestvirishvili, M.J. Miller, A. Moeller, J. Nachtman, C.R. Newsom, E. Norbeck, J. Olson, Y. Onel, F. Ozok, J. Parsons, I. Schmidt, S. Sen, J. Wetzel, T. Yetkin, K. Yi

Johns Hopkins University, Baltimore, USA

B.A. Barnett, B. Blumenfeld, A. Bonato, C.Y. Chien, D. Fehling, G. Giurciu, A.V. Gritsan, Z.J. Guo, P. Maksimovic, S. Rappoccio, M. Swartz, N.V. Tran, Y. Zhang

The University of Kansas, Lawrence, USA

P. Baringer, A. Bean, O. Grachov, M. Murray, V. Radicci, S. Sanders, J.S. Wood, V. Zhukova

Kansas State University, Manhattan, USA

D. Bandurin, T. Bolton, K. Kaadze, A. Liu, Y. Maravin, D. Onoprienko, I. Svintradze, Z. Wan

Lawrence Livermore National Laboratory, Livermore, USA

J. Gronberg, J. Hollar, D. Lange, D. Wright

University of Maryland, College Park, USA

D. Baden, R. Bard, M. Boutemour, S.C. Eno, D. Ferencek, N.J. Hadley, R.G. Kellogg, M. Kirn, S. Kunori, K. Rossato, P. Rumerio, F. Santanastasio, A. Skuja, J. Temple, M.B. Tonjes, S.C. Tonwar, T. Toole, E. Twedt

Massachusetts Institute of Technology, Cambridge, USA

B. Alver, G. Bauer, J. Bendavid, W. Busza, E. Butz, I.A. Cali, M. Chan, D. D'Enterria, P. Everaerts, G. Gomez Ceballos, K.A. Hahn, P. Harris, S. Jaditz, Y. Kim, M. Klute, Y.-J. Lee, W. Li, C. Loizides, T. Ma, M. Miller, S. Nahn, C. Paus, C. Roland, G. Roland, M. Rudolph, G. Stephans, K. Sumorok, K. Sung, S. Vaurynovich, E.A. Wenger, B. Wyslouch, S. Xie, Y. Yilmaz, A.S. Yoon

University of Minnesota, Minneapolis, USA

D. Bailleux, S.I. Cooper, P. Cushman, B. Dahmes, A. De Benedetti, A. Dolgoplov, P.R. Duderod, R. Egeland, G. Franzoni, J. Haupt, A. Inyakin³⁷, K. Klappoetke, Y. Kubota, J. Mans, N. Mirman, D. Petyt, V. Rekovic, R. Rusack, M. Schroeder, A. Singovsky, J. Zhang

University of Mississippi, University, USA

L.M. Cremaldi, R. Godang, R. Kroeger, L. Perera, R. Rahmat, D.A. Sanders, P. Sonnek, D. Summers

University of Nebraska-Lincoln, Lincoln, USA

K. Bloom, B. Bockelman, S. Bose, J. Butt, D.R. Claes, A. Dominguez, M. Eads, J. Keller, T. Kelly, I. Kravchenko, J. Lazo-Flores, C. Lundstedt, H. Malbouisson, S. Malik, G.R. Snow

State University of New York at Buffalo, Buffalo, USA

U. Baur, I. Iashvili, A. Kharchilava, A. Kumar, K. Smith, M. Strang

Northeastern University, Boston, USA

G. Alverson, E. Barberis, O. Boeriu, G. Eulisse, G. Govi, T. McCauley, Y. Musienko³⁸, S. Muzaffar, I. Osborne, T. Paul, S. Reucroft, J. Swain, L. Taylor, L. Tuura

Northwestern University, Evanston, USA

A. Anastassov, B. Gobbi, A. Kubik, R.A. Ofierzynski, A. Pozdnyakov, M. Schmitt, S. Stoynev, M. Velasco, S. Won

University of Notre Dame, Notre Dame, USA

L. Antonelli, D. Berry, M. Hildreth, C. Jessop, D.J. Karmgard, T. Kolberg, K. Lannon, S. Lynch,

N. Marinelli, D.M. Morse, R. Ruchti, J. Slaunwhite, J. Warchol, M. Wayne

The Ohio State University, Columbus, USA

B. Bylsma, L.S. Durkin, J. Gilmore³⁹, J. Gu, P. Killewald, T.Y. Ling, G. Williams

Princeton University, Princeton, USA

N. Adam, E. Berry, P. Elmer, A. Garmash, D. Gerbaudo, V. Halyo, A. Hunt, J. Jones, E. Laird, D. Marlow, T. Medvedeva, M. Mooney, J. Olsen, P. Piroué, D. Stickland, C. Tully, J.S. Werner, T. Wildish, Z. Xie, A. Zuranski

University of Puerto Rico, Mayaguez, USA

J.G. Acosta, M. Bonnett Del Alamo, X.T. Huang, A. Lopez, H. Mendez, S. Oliveros, J.E. Ramirez Vargas, N. Santacruz, A. Zatzerklyany

Purdue University, West Lafayette, USA

E. Alagoz, E. Antillon, V.E. Barnes, G. Bolla, D. Bortoletto, A. Everett, A.F. Garfinkel, Z. Gecse, L. Gutay, N. Ippolito, M. Jones, O. Koybasi, A.T. Laasanen, N. Leonardo, C. Liu, V. Maroussov, P. Merkel, D.H. Miller, N. Neumeister, A. Sedov, I. Shipsey, H.D. Yoo, Y. Zheng

Purdue University Calumet, Hammond, USA

P. Jindal, N. Parashar

Rice University, Houston, USA

V. Cuplov, K.M. Ecklund, F.J.M. Geurts, J.H. Liu, D. Maronde, M. Matveev, B.P. Padley, R. Redjimi, J. Roberts, L. Sabbatini, A. Tumanov

University of Rochester, Rochester, USA

B. Betchart, A. Bodek, H. Budd, Y.S. Chung, P. de Barbaro, R. Demina, H. Flacher, Y. Gotra, A. Harel, S. Korjenevski, D.C. Miner, D. Orbaker, G. Petrillo, D. Vishnevskiy, M. Zielinski

The Rockefeller University, New York, USA

A. Bhatti, L. Demortier, K. Goulianos, K. Hatakeyama, G. Lungu, C. Mesropian, M. Yan

Rutgers, the State University of New Jersey, Piscataway, USA

O. Atramentov, E. Bartz, Y. Gershtein, E. Halkiadakis, D. Hits, A. Lath, K. Rose, S. Schnetzer, S. Somalwar, R. Stone, S. Thomas, T.L. Watts

University of Tennessee, Knoxville, USA

G. Cerizza, M. Hollingsworth, S. Spanier, Z.C. Yang, A. York

Texas A&M University, College Station, USA

J. Asaadi, A. Aurisano, R. Eusebi, A. Golyash, A. Gurrola, T. Kamon, C.N. Nguyen, J. Pivarski, A. Safonov, S. Sengupta, D. Toback, M. Weinberger

Texas Tech University, Lubbock, USA

N. Akchurin, L. Berntzon, K. Gumus, C. Jeong, H. Kim, S.W. Lee, S. Popescu, Y. Roh, A. Sill, I. Volobouev, E. Washington, R. Wigmans, E. Yazgan

Vanderbilt University, Nashville, USA

D. Engh, C. Florez, W. Johns, S. Pathak, P. Sheldon

University of Virginia, Charlottesville, USA

D. Andelin, M.W. Arenton, M. Balazs, S. Boutle, M. Buehler, S. Conetti, B. Cox, R. Hirosky, A. Ledovskoy, C. Neu, D. Phillips II, M. Ronquest, R. Yohay

Wayne State University, Detroit, USA

S. Gollapinni, K. Gunthoti, R. Harr, P.E. Karchin, M. Mattson, A. Sakharov

University of Wisconsin, Madison, USA

M. Anderson, M. Bachtis, J.N. Bellinger, D. Carlsmith, I. Crotty¹, S. Dasu, S. Dutta, J. Efron, F. Feyzi, K. Flood, L. Gray, K.S. Grogg, M. Grothe, R. Hall-Wilton¹, M. Jaworski, P. Klabbers, J. Klukas, A. Lanaro, C. Lazaridis, J. Leonard, R. Loveless, M. Magrans de Abril, A. Mohapatra, G. Ott, G. Polese, D. Reeder, A. Savin, W.H. Smith, A. Sourkov⁴⁰, J. Swanson, M. Weinberg, D. Wenman, M. Wensveen, A. White

†: Deceased

1: Also at CERN, European Organization for Nuclear Research, Geneva, Switzerland

2: Also at Universidade Federal do ABC, Santo Andre, Brazil

3: Also at Soltan Institute for Nuclear Studies, Warsaw, Poland

4: Also at Université de Haute-Alsace, Mulhouse, France

5: Also at Centre de Calcul de l'Institut National de Physique Nucleaire et de Physique des Particules (IN2P3), Villeurbanne, France

6: Also at Moscow State University, Moscow, Russia

7: Also at Institute of Nuclear Research ATOMKI, Debrecen, Hungary

8: Also at University of California, San Diego, La Jolla, USA

9: Also at Tata Institute of Fundamental Research - HECR, Mumbai, India

10: Also at University of Visva-Bharati, Santiniketan, India

11: Also at Facolta' Ingegneria Universita' di Roma "La Sapienza", Roma, Italy

12: Also at Università della Basilicata, Potenza, Italy

13: Also at Laboratori Nazionali di Legnaro dell' INFN, Legnaro, Italy

14: Also at Università di Trento, Trento, Italy

15: Also at ENEA - Casaccia Research Center, S. Maria di Galeria, Italy

16: Also at Warsaw University of Technology, Institute of Electronic Systems, Warsaw, Poland

17: Also at California Institute of Technology, Pasadena, USA

18: Also at Faculty of Physics of University of Belgrade, Belgrade, Serbia

19: Also at Laboratoire Leprince-Ringuet, Ecole Polytechnique, IN2P3-CNRS, Palaiseau, France

20: Also at Alstom Contracting, Geneve, Switzerland

21: Also at Scuola Normale e Sezione dell' INFN, Pisa, Italy

22: Also at University of Athens, Athens, Greece

23: Also at The University of Kansas, Lawrence, USA

24: Also at Institute for Theoretical and Experimental Physics, Moscow, Russia

25: Also at Paul Scherrer Institut, Villigen, Switzerland

26: Also at Vinca Institute of Nuclear Sciences, Belgrade, Serbia

27: Also at University of Wisconsin, Madison, USA

28: Also at Mersin University, Mersin, Turkey

29: Also at Izmir Institute of Technology, Izmir, Turkey

30: Also at Kafkas University, Kars, Turkey

31: Also at Suleyman Demirel University, Isparta, Turkey

32: Also at Ege University, Izmir, Turkey

33: Also at Rutherford Appleton Laboratory, Didcot, United Kingdom

34: Also at INFN Sezione di Perugia; Universita di Perugia, Perugia, Italy

35: Also at KFKI Research Institute for Particle and Nuclear Physics, Budapest, Hungary

36: Also at Istanbul Technical University, Istanbul, Turkey

37: Also at University of Minnesota, Minneapolis, USA

38: Also at Institute for Nuclear Research, Moscow, Russia

39: Also at Texas A&M University, College Station, USA

40: Also at State Research Center of Russian Federation, Institute for High Energy Physics, Protvino, Russia

